

Establishment of polarities in the oocyte of *Xenopus laevis*: the provisional axial symmetry of the full-grown oocyte of *Xenopus laevis*

G. A. Ubbels

*Hubrecht Laboratory, Netherlands Institute for Developmental Biology, Uppsalalaan 8,
NL-3584 CT Utrecht (The Netherlands), Fax +31 302516464*

Abstract. We aimed at understanding of formation and function of the “Nieuwkoop Centre” in embryonic pattern formation. Discussed are data on genesis of cytoplasmic localizations in ovarian oocytes, transient modifications of cytoskeletal structures creating cytoplasmic asymmetries in fertilized eggs, the axis determining “vegetal cortical rotation” and fate of distinct cells, as shown by injection of specific molecular markers into particular blastomeres at specific times. Egg rotation and centrifugation suggested that sperm that gravity cooperate in symmetrization of the axially symmetrical anuran egg. After fertilization in space or in a fast rotating clinostate, axis formation and embryonic development were normal although the blastocoel was transiently abnormal. Normal tadpoles came back on Earth after ovulation, fertilization and culture in space. They metamorphosed normally and got healthy Earth-born F₁ offspring. We conclude that neither sperm nor gravity are required for determination of the bilateral symmetry in the embryo of *Xenopus laevis*. In normal development sperm and gravity, either alone or in collaboration, may overrule an initial bilaterality inherent to the full-grown oocyte, residing in some still unidentified component(s) or mechanisms.

Key words. Anurans; *Xenopus laevis*; symmetrization; axis formation; localizations; dorso-ventral; gravity; microgravity; space shuttle; clinostate.

Introduction

In the provisionally radially symmetrical mature *Xenopus* egg, the animal-vegetal (A/V) axis of polarity roughly foreshadows the main body axis of the embryo [1–4]. However the egg needs cue(s) for the establishment of additional polarities, which are a prerequisite for normal development [5, 6]. As in many species, the sperm acts as such a cue in the monospermically fertilized *Xenopus* egg. It initiates the formation of a huge microtubule entity, the spermaster [6–9], which in its turn initiates and directs yolk shifts in the animal hemisphere, concomitantly with pigment shifts leading to grey crescent formation, thus creating bilateral symmetry before first cleavage [6, 10]. When Pieter Nieuwkoop framed his hypothesis on mesoderm induction [11] clear yolk shifts in the vegetal hemisphere of the uncleaved *Xenopus* egg were unknown, except for the formation of the vitelline wall opposite the sperm entry point (SEP) [6, 12, 13] and the accumulation of germ plasma in sub-cortical islands in the region of the vegetal pole [14, 15].

In 1969 Pieter Nieuwkoop launched his now classic hypothesis on mesoderm induction in urodelian amphibians [11], suggesting that the formation of the mesoderm in the ectodermal (=animal) hemisphere is induced by signals from the endodermal (=vegetal) half. Nieuwkoop and coworkers later published additional experimental evidence [16–19], and could generalize the hypothesis by demonstrating that it also holds

for anuran embryos [20]. Supporting evidence came from several Japanese studies [21, 22; see 18, 23 for reviews].

It is now generally accepted that mesoderm induction gives rise to early embryonic pattern formation in the amphibian embryo from the mid-blastula stage onwards. The blastocoel plays a crucial role in mesoderm induction, since the entire mesoderm originates epigenetically from the ectodermal half of the blastula under inducing influences emanating from the endodermal yolk mass [17, 18, 24]. The blastocoel develops through fusion of the progressively extending intercellular spaces between the initial four blastomeres [25, 26]. The zone of interaction is thereby restricted to the ring-shaped marginal zone, i.e. the outer equatorial zone of the blastula. Abnormal blastocoel formation could therefore interfere with axis formation [27, 28].

The interests of the more morphologically oriented experimental embryologists and molecular developmental biologists joined fruitfully in unravelling the molecular and cell biological principles underlying these phenomena, by application of microscopical, immunocytochemical and molecular biological techniques. The aim of the present volume is to summarize some of the most important data obtained so far, which support the hypothesis of mesoderm induction, trying to explain how the ‘Nieuwkoop Centre’ [1], residing in the dorsal-most vegetal cells of the early blastula, can induce the ‘Spemann organizer’ [29] which in its turn governs gastrulation and induction and patterning of the neural plate [2].

Many of these studies concentrate on the identification of factors involved in mesoderm induction, among them peptide growth factors, including fibroblast growth factors (FGFs), TGF β family members and activins, and specific maternal mRNAs like vegetal 1 (Vg1) [30, 31] and Noggin [32, 33]. Peptide growth factors and homeobox genes interact and contribute to determining the pattern and the fate of the embryonic cells [22, 34]. In this contribution we will review some relevant data concerning development before formation of the Nieuwkoop centre, i.e. in the ovarian oocyte and in the newly fertilized egg.

Many studies on embryonic axis formation in *Xenopus laevis* start from the view that the full-grown oocyte (stage 6 [35]) is radially symmetrical about the polar an/veg axis. However full-grown ovarian oocytes like those of *Ambystoma mexicanum* [35a] and *Rana esculenta*, and unfertilized eggs of *Discoglossus pictus* and *Rana esculenta*, already exhibit signs of bilateral symmetry [3, 4, 10]. We will discuss the localisation of various yolk components at particular times during vitellogenesis and the involvement of cytoskeletal modifications in the final patterning of the full-grown, seemingly axially symmetrical stage VI [35, 35b] *Xenopus oocyte*, the breaking of that axial symmetry at fertilization and the role of sperm penetration by initiating cytoplasmic segregation in the animal hemisphere and, half-way through the first cell cycle, a rotation of the vegetal cortex. Both of these mechanisms function in the rearrangement of various yolk components into a bilaterally symmetrical distribution which foreshadows the ultimate body structure of the embryo (plate I).

The formation of cytoplasmic domains could be an important determinative mechanism in early *Xenopus* development [36–40]. Specific cytoskeletal proteins with associated mRNAs [37] could function in targeted protein synthesis [38] in *Xenopus* oocytes and embryos and thus act in the formation of such cytoplasmic domains [36, 39]. Several transforming growth factor-beta (TGF- β)-like growth factors, RNA-binding proteins and a mitochondrial ATPase subunit are localized in cleavage stage embryos. Blastomere isolation and recombination studies [2, 17, 41–45] revealed differences in differentiation properties among the various blastomeres during early development, even at the 8-cell stage [46–48].

Experimental evidence exists that the sperm is *not* required for axis formation in *Xenopus laevis*, though it cues the cortical rotation which is essential for the symmetrization [1, 49, 50]. In the anuran *Discoglossus pictus* the sperm penetrates into the egg near to the animal pole it induces cytoplasmic segregation which symmetrizes the egg during the pre-cleavage period and, as in *Xenopus*, foreshadows the definite body axis of the embryo [51].

As in most anurans [4], the *Xenopus* egg rotates upon sperm penetration, turning its animal-vegetal axis up-

right ('rotation of orientation') [52, 53], and the blastopore tends to form opposite the sperm entry point (SEP), but this only holds for about 70% of the embryos [12, 54], suggesting that some additional unknown factor(s) are involved in axis formation. Classical experiments [e.g. 52, 55–59; 4 for review] including egg rotation and centrifugation, suggested that gravity is at work in the determination of the spatial structure of the amphibian embryo, for instance by cooperating with the sperm in initiating yolk shifts. However, because of the lack of suitable methods and proper surroundings, it was impossible to test this hypothesis in a proper way, i.e. in near-weightlessness [60]. Only in 1985 did it become possible to perform such an experiment in actual microgravity (μ g) under well-controlled conditions in the Biorack in the Space Lab [61, 62] and, from 1988 onwards, during sounding rocket flights [63–65] and during additional space shuttle missions (table 1 and ref. 65a).

In egg rotation and centrifugation experiments with fertilized eggs the cueing action of the sperm can be overruled by gravity or centrifugal forces (plate II: J and K). Gravity could thus play a part in the natural symmetrization process [5, 12, 54, 60, 66–68]. However, experiments under conditions of actual and simulated microgravity (table 1, plate II) revealed that gravity is not required for dorso-ventral polarization [27, 28], nor for embryonic pattern formation, since after fertilization and culture in microgravity normal tadpoles and larvae still formed [69].

Neither sperm [49, 50] nor gravity [27, 28, 69] are required for determination of the bilateral symmetry in the embryo of *Xenopus laevis* [50]. We will argue that, in normal development, both the penetrating sperm and gravity, either alone or in collaboration, may overrule an initial bilaterality inherent to the full-grown oocyte, which resides in some component(s) and/or mechanism(s) which are still unidentified. The radial symmetry of the full-grown, mature oocyte is probably only provisional. This idea is supported by more recent data [70].

The genesis of the full-grown oocyte

During vitellogenesis the post-replicative oocyte is arrested in meiotic prophase I. Mitochondria, yolk granules and other cell constituents such as mRNAs, structural proteins and possibly morphogenetic determinants accumulate in distinct regions of the ovarian oocyte [4, 37, 38] and, as oogenesis progresses, are redistributed into distinct configurations and gradients [1, 49]. A provisional radial symmetry of the full-grown oocyte about its animal-vegetal axis is expressed e.g. by the localization of the nucleus, the pigment pattern, and the spatial distribution of yolk platelets, mitochondria, cortical granules and many other cytoplasmic con-

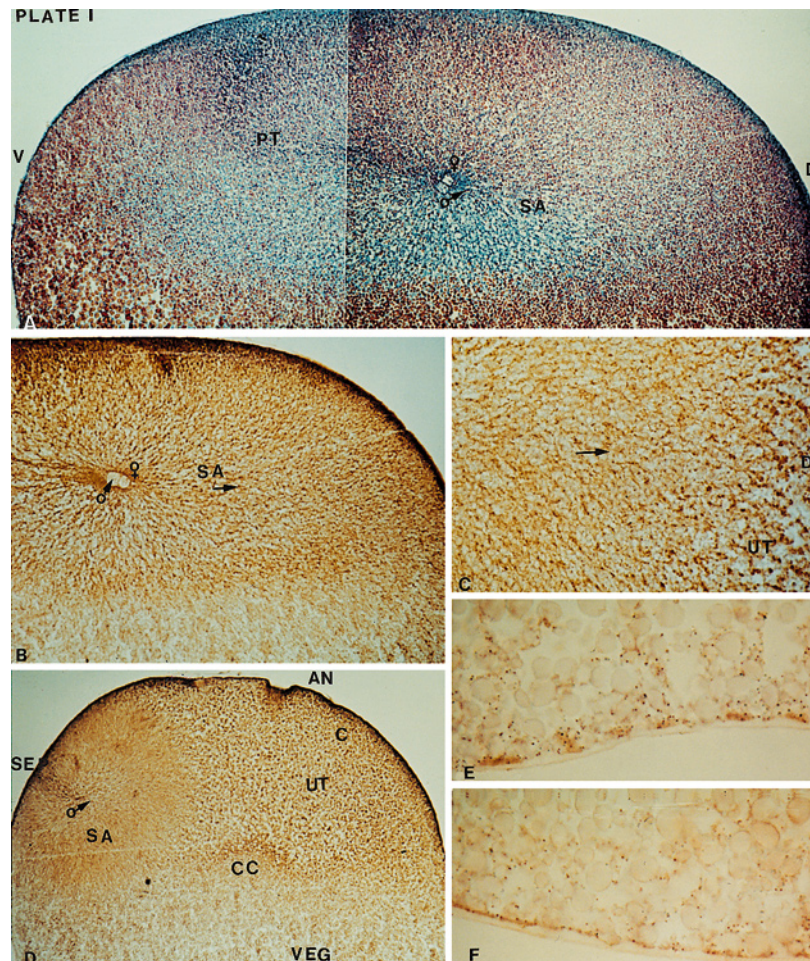


Plate I. Cytoplasmic segregation and microtubules in pre-cleavage eggs of *Xenopus laevis*. (A) Median 6 μm paraffin section through the SEP and the animal-vegetal axis of a NT 0.6 *Xenopus* egg, fixed in Bouin d'Hollande, stained by azofuchsin, anilin blue and orange G [6]. Animal hemisphere with (σ) male and (φ) female pronucleus, closely associated, but not yet fused. Different sizes of red yolk granules, rearranging themselves under the influence of the penetrating sperm, whose path is marked by the pigment trail (PT). SA = blue stained spermaster rays; nuclei shifted slightly dorsally. D = dorsal, V = ventral. (B–F) Distribution of polymerized and unpolymerized tubulin in fertilized *Xenopus* eggs. Yolk granules unstained under the conditions chosen (Bouin d'Hollande fixation; 6 μm paraffin section; modified PAP-staining, using anti-tubulin MABs [82, 83a, 86, 184]. Dorsal half of NT-0.66 *Xenopus* egg (cf. A). (C) detail of (B). SA = spermaster; DC = dorsal cytoplasm, not shown in (B) but present in adjacent sections (cf. C); UT = unpolymerized tubulin; AN = animal; VEG = vegetal. (D) NT-0.2; 6 μm median section through the SEP and animal-vegetal axis. CC = central cytoplasm. (E, F) Genesis of vegetal cortical array in fertilized eggs: (E) *Xenopus* egg; at NT-0.2 distinct patches stain in the cortex of the vegetal hemisphere. These expand progressively and at NT-0.6 merge into a continuous layer (F). The immunocytochemical staining with tubulin MABs, and appropriate controls (not shown), reveal that the patches and the layer contain tubulin and probably reflect the genesis of the vegetal microtubule array.

stituents like mRNAs and cytoskeletal structures [6, 10, 13, 30, 35, 71–77, 83; 3 for review]. After dramatic changes in the intracellular organization during maturation [4, 25, 78, 78a], the oocyte reaches the second metaphase and is ready for fertilization [79]. The primary, i.e. A/V, polarity of the full-grown amphibian oocytes and mature eggs foreshadows the spatial structure of the embryo [1, 4]. By definition the second meiotic spindle marks the animal pole, while the vegetal pole is 180 degrees away from the animal pole. The animal pole is the centre of the pigmented animal hemisphere, marked by the depigmented maturation spot [10, 26]. Recent research [70] has shown that the centre of the maturation spot is situated on average at 15 degrees or

more from the geometric animal pole. It is suggested that this originates from an off-axis oocyte orientation during oogenesis, and that the eccentric maturation spot position determines the future alignment of the cortical microtubules guiding the vegetal yolk mass rotation following egg activation. The vegetal pole is often surrounded at some distance by a ring of pigment [25, 26] in the centre of the vegetal hemisphere.

There is no other evidence for an external source of the A/V polarity in the *Xenopus* oocyte, such as blood supply, gravity or a topographic relationship of egg axis and follicle cells [50; 4 for review]. On the other hand, actin transcripts are expressed in follicle cells and *Xenopus* oocytes; actin βA and possibly βB polypep-

Table 1. Fertilization and development of eggs of *Xenopus laevis* experiments in actual and simulated microgravity.

<i>A. Simulated microgravity on a fast-rotating clinostate</i>	
a)	Fertilization at 1g; selected eggs in the clinostate after rotation of orientation.
b)	Fertilization, i.e. mixing of eggs and sperm in the clinostate, just prior to the start of clinostating.
<i>B. Actual microgravity during a sounding rocket (SR) flight (6–7 min μg)</i>	
a)	Both fertilization and histological fixation in μ g (TEXUS-17).
b)	Fertilization in μ g, histological fixation either in μ g or after retrieval and 5 days' culture at 1g on Earth (MASER-3).
c)	Fertilization 5'30" before launch; video recording before launch and in flight; fixation after retrieval and embryo culture on Earth, i.e. at 1g, for different periods (MASER-6).
d)	Fertilization at 0g and in a 1g centrifuge in flight; culture on Earth after retrieval, and histological fixations at different time intervals, e.g. as gastrulae (analysed by in situ hybridization with an <i>X-bra</i> probe) and various larval stages (MASER-6).
e)	Fertilization on Earth after retrieval, histological fixations at different time intervals (MASER-6).
<i>C. Pulses of actual microgravity, i.e. 31 parabolas during a parabolic flight (COLCAMP 2)</i>	
a)	Fertilization in a flight of 2.5 h, with regular intervals during five different parabolas and immediately after retrieval; as control: on Earth, shortly before flight. All embryos were grown on Earth and histologically fixed at different intervals after retrieval.
<i>D. Actual microgravity in the American space shuttle (7–9 days)¹</i>	
a)	Both fertilization and histological fixation in automated experiment containers at the gastrula stage, both in μ g and in the 1g centrifuge aboard (IML-1).
b)	Ibid. at the eighth cleavage in automated experiment containers (IML-2).

¹These experiments were performed in automated experiment containers; each allowed us harvest one or more 'space first(s)'.

tides synthesized in follicle cells are secreted and then taken up by the oocytes, whereas activin β B2 might be synthesized in the oocytes [80]. In the full-grown oocyte this could initiate cytoplasmic asymmetries of developmentally important molecules.

The development of the cytoskeleton in ovarian oocytes and fertilized eggs has recently been analyzed extensively by confocal immunofluorescence microscopy and immunocytochemistry. The distribution of the tubulin structures in ovarian oocytes [77] and in newly fertilized eggs [3, 74, 81, 82, 82a] compared to those of mitochondria (cf. fig. 19 in [83]) and yolk granules (plate I and refs [6, 10, 77, 82, 84–86; 3 for review] make it conceivable that microtubules (MTs) function in localization of visible cell constituents along with other cell components [87, 88], to direct and start synthetic processes at particular times and places [36].

Genesis and localization of yolk bodies in the ovarian oocyte

The primary polarity of the full-grown oocyte is clearly expressed by the regional differences in yolk composi-

tion [1–3, 6, 10; 4 for review]. The genesis of the yolk pattern in ovarian oocytes has been studied extensively by Danilchik and Gerhart et al. [49, 50]. Most of the yolk granules form from vitellogenin, an external precursor protein synthesized in the liver and transported via the blood stream to the ovary, where it is taken up by the oocytes through receptor mediated pinocytosis [89; 4 for review]. In the oocyte, the vitellogenin is temporarily contained in 'transitional yolk bodies' which then either fuse with preexisting platelets forming larger entities, or initiate the formation of new yolk bodies. Gerhart et al. [49, 50] started their analysis by preparing fluorescent derivatives of vitellogenin which were injected into the frog's dorsal lymph sac, thus entering the blood stream and finally reaching the oocytes in the ovary. Both the transformed older and the newly formed yolk bodies became fluorescently labelled and their location could easily be detected in histological sections with the aid of fluorescence and polarization microscopy (fig. 1 and legend; after ref. 50, modified). By comparing sections from 1.2 mm oocytes (stage V and VI [35]) isolated from the ovary 1, 3, 5, 10 or 19 days after the injection with the fluorescently labelled vitellogenin, the front of fluorescent platelets could be determined and was found to go progressively inwards with time. There was no local difference in the rates of uptake of fluorescently or radioactively labelled vitellogenin across the oocyte surface, but a considerable amount of yolk is translocated intracellularly from the animal towards the vegetal side, a process most likely mediated by the cytoskeleton. The vegetal half of the full-grown oocyte ultimately contains about two-thirds of the yolk.

Genesis and distribution of mitochondria and microtubules in ovarian oocytes

The 'Balbani body' [90] or 'Balbani vesicle' plays an important role in the determination of the axial symmetry of ovarian oocytes in many species [91, 91a for reviews]. After four cell divisions, *Xenopus* oogonia do express a clear polarity which is visible due to the alignment of nucleus, centrosome and the incomplete division bridge [4, 50, 83, 92–94, 94a]. This polarity could foreshadow the A/V axis, the side of the nucleus becoming the future animal pole [50]. In early stage I (80 μ m) oocytes [35, 35b], small mitochondrial masses are first dispersed around the germinal vesicle (GV), condense and then form a cap-like structure at one side of the GV which stains with basophilic dyes and which faces towards the future vegetal pole region [91]. Thereafter this structure disperses, forming the 'mitochondrial cloud' [92] which, as shown by TEM, contains mitochondria and electron-dense granulofibrillar materials (part of) which were suggested [94] to become components of the germinal cytoplasm [14].

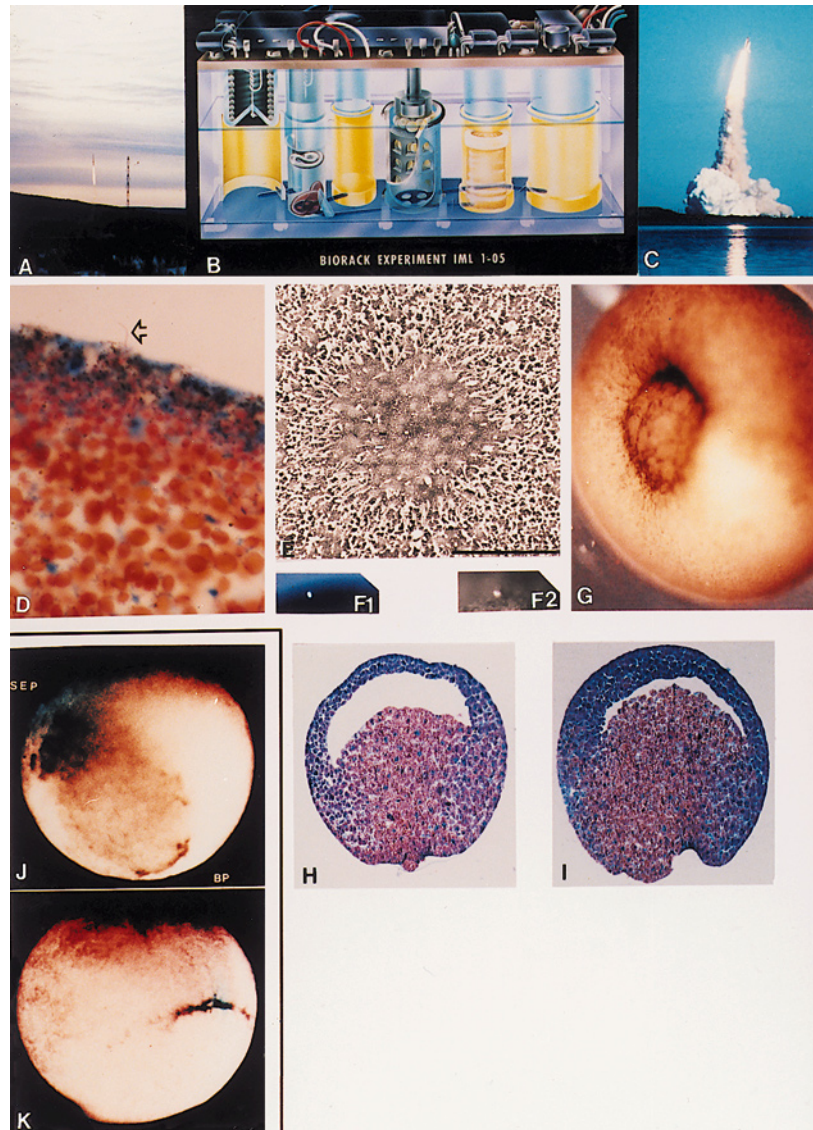


Plate II. Egg rotation and microgravity experiments during early *Xenopus laevis* development. (A) Launch sounding rocket SR-TEXUS17, May 2, 1988 (ESRANGE, Kiruna, Sweden). (B) Automated experiment container (AEC) used in the sounding rocket missions on SR-TEXUS-17 and SR-MASER-3, and the IML-1 mission of space shuttle 'Discovery', January 22–30, 1992 (Kennedy Space Center, Florida, USA). For explanation: p. 397 (fig. 7 and legend). (C) Launch American space shuttle for the IML-1 mission. (D) Median 6 μm histological paraffin section through the SEP and the animal-vegetal axis of *Xenopus* egg with penetrating sperm, fixed 2'55" min after automated fertilization in μg [176]. (E) Frequently observed smooth surface area, surrounded by a concentration of microvilli often with a clump of microvilli in the centre, probably an abortive penetration [175]. SEM photograph of egg, 2'55" [176], after automated fertilization and subsequent fixation in 3% buffered glutaraldehyde (GA), in μg . Vitelline membranes were manually removed. (F1) and (F2) UV-fluorescence of penetrating sperm: 1) 3 min p.f., unfixed egg, fertilized in Hoechst 33258; 2) egg in μg on SR-M3, automated fertilization after 6 h pre-incubation in Hoechst-33258, fixed 4'35" min. p.f. in 3% buffered glutaraldehyde; vitelline membranes manually removed. (G) A 'space first' from IML-1: for the very first time gastrulae developed in space, from eggs fertilized in space. Automated fertilization at 22.5 °C, 24 h after stripping; histologically fixed 12 h later, in 3% glutaraldehyde in 25% MMR; return to Earth after seven days. BP = blastopore. (H, I) 6 μm histological section, fixed after automated delayed fertilization in the Biorack on Earth (H), or during flight (I). Compared to the H-gastrulae from the 1g centrifuge in flight and the Biorack on Earth, the roof of the blastocoel is thicker, and the blastocoel is smaller in most of the μg -gastrulae (I). (J, K) Egg rotation experiment. Whole mounts of early *Xenopus* gastrulae, fixed at stage X [26], (J) with blastopore (BP) opposite the sperm entry point (SEP); (K) reversed BP, after egg rotation through 90 degrees before first cleavage, with SEP-up: BP forms on the SEP meridian (cf. fig. 5 and refs 12, 54).

The total number of mitochondria progressively increases during oocyte growth, scattered randomly in the cytoplasm of ovarian oocytes [35], and the embryo is ultimately provided with a huge number of maternal mitochondria. In oocytes of about 250–275 μm , at the beginning of vitellogenesis, the mitochondrial mass splits

up into two different non-randomly distributed populations. Along with the formation of yolk platelets and ribosomes, this process correlates with the biogenesis of the final amount of mtDNA in the full-grown oocyte [83, 94a]. The proximal mass first surrounds the nucleus, and in oocytes of about 750 μm , forms a crown at

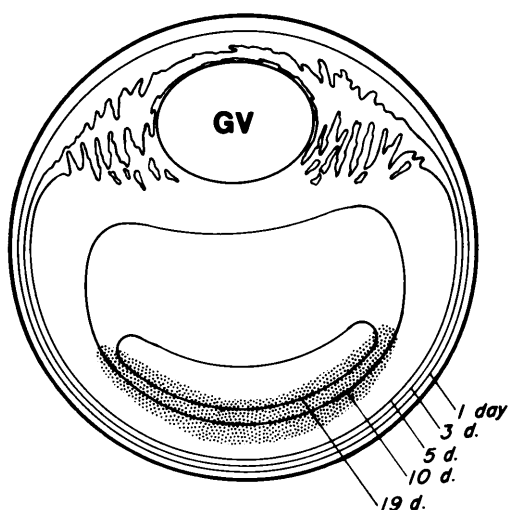


Figure 1. The temporal-spatial pattern of yolk platelet formation in the *Xenopus* oocyte. Diagram of a cross-section of full-grown oocyte (1.2 mm diameter) [49, 50]. Most of the yolk granules form from vitellogenin, an external precursor protein synthesized in the liver, transported via the blood stream to the ovary, and taken up by the oocytes through receptor-mediated pinocytosis. In the oocyte, the vitellogenin is temporarily contained in 'transitional yolk bodies' which either fuse with preexisting platelets, or initiate the formation of new yolk bodies. Fluorescent derivatives of vitellogenin [50] injected into the frog's dorsal lymph sac enter the oocytes in the ovary via the blood stream. Both transformed older and newly formed yolk bodies become fluorescently labelled and can easily be detected in histological sections with fluorescence and polarization microscopy. By comparing sections from 1.2 mm oocytes (stage V and VI [35], isolated from the ovary 1, 3, 5, 10 or 19 days after injecting fluorescently labelled vitellogenin) the front of fluorescent platelets could be determined and was found to go progressively more interior with time, moving more rapidly through the animal hemisphere than the vegetal hemisphere. There is no local difference in the rates of uptake of fluorescently or radioactively labelled vitellogenin across the oocyte surface, but a considerable amount of yolk is translocated intracellularly, from the animal towards the vegetal side, a process most likely mediated by the cytoskeleton. The vegetal half of the full-grown oocyte ultimately contains about two-thirds of the yolk. After Gerhart et al. [50]; modified with permission; cf. also ref. 49. (Reprinted with permission from: Gerhart J. et al. (1986) Primary and Secondary Polarity of the Amphibian Oocyte and Egg. In: Gametogenesis and the Early Embryo, pp. 305–319, John Wiley & Sons, Inc., New York).

one side of the nucleus; the more distal mass in oocytes of about 800 μm ultimately forms a continuous layer of mitochondria under the plasmalemma of the entire vegetal hemisphere. The crown population is always less compact than the mitochondrial mass, though [94a] the density of organelles in each population remains the same until about halfway through st.V [35]. The two populations show a different affinity for toluidine blue; thymidine incorporation is always strongest in the crown population. Mitochondrial biogenesis was always found in the vicinity of the nucleus, i.e. in previtellogenic oocytes in the mitochondrial mass and in vitellogenic oocytes in the nuclear crown.

Such a localization of two spatially different populations of mitochondria (mt) [92, 94] through oogenesis was confirmed in a recent in situ hybridization analysis

of the distributions of mt l-r RNAs (large ribosomal subunit (16S) RNAs) [95]. mt l-r RNAs were found in the Balbiani body and in small perinuclear clumps in stage I oocytes; in the larger previtellogenic (stage III) oocytes the perinuclear distribution of mitochondria persisted, while the greatest accumulation of mitochondria was present in the yolk-free cytoplasmic region at the vegetal base of the germinal vesicle, which forms the boundary between regions with different classes of yolk platelets. During maturation this zone spreads and separates the animal hemisphere cytoplasm from the vegetal yolk mass [96] and after fertilization the asymmetric distribution of mitochondria in the egg cytoplasm is still further enhanced [84, 95].

Cytoskeletal structures guide the distribution of cell components. Cytoplasmic microtubules are organized in a network in all oocyte stages; many tiny foci present in the cytoplasm of early oocytes are distinguishable in older oocytes as small clusters of microtubules. Microtubules form a distinct boundary around and also penetrate into the Balbiani body [77, 82a]. The anti-tubulin immunofluorescence in early oocytes showed a close association of centrosome and Balbiani body [77, 82a], suggesting that the Balbiani body functions as a microtubule organizing centre (MTOC) [82a, 93].

Only recently could many active centrosomes in stage 0 (12–25 μm) and stage I (30–50 μm) oocytes [35] be shown to stain strongly with antibodies to γ -tubulin (γ -TB), a centrosomal protein [91a, 97, 97a]. Whether centrosome and Balbiani body remain associated when the latter moves to its eccentric position, and then functions as an organizing centre in the vegetal hemisphere, is not known [81, 82a, 98]. In the peripheral cortex and the perinuclear region the microtubule network is rather dense [81], much γ -tubulin is asymmetrically distributed in the cortex of stage VI oocytes [74]. From stage II onwards, strongly fluorescent quasi-radial structures, presumably bundles of microtubuli, form in the cytoplasm of vitellogenic oocytes. Starting from the region of the disintegrated mitochondrial mass they progressively fill the entire region between the germinal vesicle and the cortex of the oocyte. In stage III an extremely strongly fluorescent belt becomes apparent in the ring-shaped perinuclear area. The organization of microtubules in the prospective animal and vegetal hemispheres progressively becomes more distinct from stage IV onwards.

By the end of vitellogenesis (stage VI), the quasi-radially arranged tubulin-containing structures radiate from the vicinity of the nucleus towards the oocyte's periphery in the entire animal hemisphere only, while a cap or basket-like region of tubulin-rich cytoplasm surrounds the nucleus at the side facing the future vegetal half of the oocyte. Numerous microtubules are embedded in the amorphous matrix of the perinuclear cap, and both matrix and microtubules extend into clefts or in between

protuberances of the nuclear envelope [82a]. In confocal laser scanning microscopy (CLSM) pictures many of these microtubules were continuous with cytoplasmic MT bundles, suggesting that in stage VI the germinal vesicle operates as a MTOC [81, 82a].

Differential distribution of mRNAs in ovarian oocytes

Maternal mRNAs can be spatially localized in animal and vegetal regions of the provisionally radially symmetrical *Xenopus* oocyte [30, 31]. Xcat2 mRNA was found localized in the mitochondrial cloud and subsequently anchored to the vegetal cortex [87]. In stages I and II oocytes at least three mRNAs, viz. Xlsrts, Xcat2 and Xwnt11, were localized within a special region of the mitochondrial cloud, functioning as a METRO (i.e. 'message transport organizer'), and translocated towards a restricted region of the vegetal cortex around the vegetal pole [99]. These mRNAs anchor at the vegetal cortex in an overlapping layered pattern, in such a way that Xcat2 is closest to the cortex, overlapped sequentially more inwardly by Xlsrts and Xwnt11. This localization process thus involves accumulation and sorting of mRNAs within the mitochondrial cloud as well as anchoring to the vegetal cortex by cytoskeletal elements. The route of Vg1 mRNA is different, since it follows a pathway outside of the cloud. Vg1 mRNA is evenly distributed in the cytoplasm during stage II, but during stage III it translocates through the cytoplasm, using the same route as the METRO before, and is completely localized at stage IV, to the same cortical position as the METRO-localized mRNAs [99]. The translocation of Vg1 involves association with microtubules [100], its anchoring depends on actin microfilaments [99–101] which form a network that anchors it to the vegetal cortex, and which also includes putative structural RNAs. After tight association of Vg1 with the vegetal cortex and overlapping Xlsrts in stage IV oocytes, Vg1 spreads along the inner cortical region approximately up to about the equatorial region, reaching the future marginal zone [99]. The proper localization of Vg1 and Vg1-like RNAs may depend on the formation of a cytoskeletal pathway by the mitochondrial cloud, and this may contribute to axis determination [99, 102]. Vg1, Xcat-2 and Xcat-3 mRNAs were also specifically retained in isolated pieces of the vegetal cortex of stage VI oocytes [103]. These data suggest that the cortex of the region around the vegetal pole represents a unique structure with a specialized cytoskeletal domain, which retains various localized mRNAs [103a,b]. It could function in the determination of the primary polarity of the full-grown *Xenopus* oocyte [2, 3].

The newly fertilized egg during the first cell cycle

Morphological phenomena started by sperm penetration

Only one sperm penetrates at random, and into the

pigmented animal hemisphere only [10, 13, 104]. Its penetration raises a transient electrical block against polyspermy and initiates the *activation wave* (AW), the first visible expression of dorso-ventral polarity. The AW is a surface wave which, as can be visualized by video time-lapse recording, proceeds from the SEP over the egg surface at a speed of about 10 $\mu\text{m}/\text{sec}$, reflecting the extrusion of the cortical granules, which loosens the vitelline membrane with adhering jelly from the egg surface [6, 105]. Since the AW is sensitive to cytochalasin [6], microfilaments must be involved in the extrusion of the cortical granules. The membranes surrounding the cortical granules fuse with the egg membrane. After fertilization the cortex contracts [105a] and within 10–12 min, the egg reacts to gravity and rotates as an entity inside its vitelline membrane, turning its animal-vegetal axis upright ('rotation of orientation') [52, 53, 56, 62]. Successful fertilizations in actual [27, 28, 63, 65, 69, 106] and simulated [67, 68 and this study] microgravity (μg) showed that the rotation of orientation [52, 53] is not essential for normal development, since eggs developed normally [27, 28, 63, 69] although they did not rotate under actual microgravity (μg) conditions.

The second polar body is extruded at $\pm\text{NT } 0.25$ (NT stands for the fraction of time to first cleavage) [6]. Mutual relationships between the male and the female pronucleus, the pronuclear paths and the spermaster are most clear in saggital histological sections, i.e. in and parallel to the plane through the SEP and the animal-vegetal axis. Pigment concentrates about the SEP, marking the future ventral side, and making axis manipulation possible in early stages [10, 13, 58, 59, 107]. The path of the migrating male pronucleus (plate I, A) is marked by pigment granules, drawn into the cytoplasm from the egg surface as the sperm moves inward (NT 0.17–0.61) [6–10, 13]. The female pronucleus moves down from the animal pole, probably soon coming under influence of the spermaster [108]. Male and female pronuclei meet at about NT 0.52, and only fuse at NT 0.7–0.8 [6]; the zygote nucleus is in most embryos slightly shifted to the *dorsal* side and never, as is sometimes suggested, to the *ventral* side (cf. fig. 3 in ref. 109). As a consequence the two animal-dorsal blastomeres are smaller in most 8-cell *Xenopus* embryos [26].

During the first cell cycle two main independent microtubular entities develop: (1) the spermaster, initiated in the animal hemisphere by the sperm centriole [6, 7, 9], and (2) an array of parallel MT in the subcortical cytoplasm of the vegetal hemisphere about half-way through the first cleavage [82a, 107, 110].

In 6 μm paraffin sections of Bouin d'Hollande-fixed [77, 85, 86, 96a] *Xenopus* eggs we analyzed the three-dimensional distribution of tubulin with a modified peroxidase-anti-peroxidase (PAP) procedure [82, 82a]. The antigenic properties of tubulin remained unchanged in Bouin d'Hollande-fixed *Xenopus* eggs after alcoholic

dehydration and paraffin embedding, polymerized and unpolymerized tubulin structures were preserved (plate I, B–D; controls not shown), but broke down during vinblastine incubation. Only unpolymerized (γ) tubulin stained in VB-treated sections (not shown).

The spermaster initiates a polarized segregation of the animal cytoplasm

Fertilization initiates the formation of the spermaster, a huge three-dimensional MT entity, [6–10, 13] initiated by the sperm centriole. The spermaster progressively expands into the animal hemisphere, a process which can be visualized on the egg cortex by video time lapse recording as a *post fertilization wave* (PFW) which, like the AW, spreads from the SEP from the ventral towards the dorsal side but at 1 $\mu\text{m}/\text{sec}$ [6, 54]. The PFW is sensitive to vinblastine treatment, confirming microtubule involvement. The microtubules of the spermaster spread radially from the sperm centriole (plate I, A, B, D), lead the sperm pronucleus during its penetration, and also lead the female pronucleus as soon as it reaches the region with the outgrowing spermaster rays. The constant growth rate of the spermaster microtubules causes the male and female pronuclei to migrate at a constant rate of 12 μm per min [6, 9, 107, 111]. While the animal cortex locally contracts on the SEP side, the astral rays reach the opposite side at NT 0.65–0.8. [6, 82, 105a, 107].

From NT 0.78–0.95 onwards, the cytoplasmic microtubules in the animal half progressively depolymerize, starting from the SEP side, and around NT 0.80 only remnants of astral microtubules are present [6, 82, 82a]. The vegetal cortical array of parallel microtubules persists until first cleavage when new mitotic microtubules form, first only in a restricted part of the dorsal hemisphere, but progressively accumulating in the entire ventral half and gradually extending into the entire animal hemisphere and finally reaching the cortex [6, 82a].

These observations tally well with biochemical analyses [112], which showed that at about the time of metaphase (0.85 NT) in the zygote large amounts of tubulin polymers break down and reappear at the time of first cleavage (1.0 NT).

Additional transient spherically distributed (bundles of) thin microtubules may direct transport of cytoplasmic components

In between the relatively coarse spermaster rays thin tubulin fibrils were also observed. These became progressively longer with time, measuring $\pm 20 \mu\text{m}$ at NT 0.2, $\pm 110 \mu\text{m}$ at NT 0.35 [82, 86]. From then on, these tubulin fibrils did not lengthen any further, but were visible in the sections in a region which progressed dorsally with time as a spherical wave front (plate I, B–D), suggesting that these thin fibrils moved as enti-

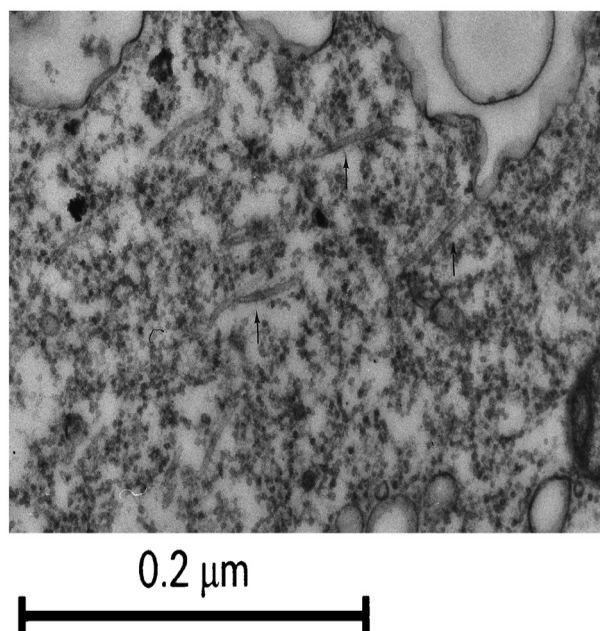


Figure 2. TEM picture of the centre of the dorsal yolk-free cytoplasm in the egg of *Xenopus laevis*, NT 0.66 (bar is 0.2 μm). Occasionally relatively long, and very often parallel, microtubules are present (\uparrow). The DYFC [6, 10, 84] has morphological characteristics of a metabolically active region. Microtubules were absent when fixed in a mixture of 1% acroleine and 2.5% glutaraldehyde in 0.067 M cacodylate buffer (pH 7.2), post-fixed in 2% osmium tetroxide in cacodylate buffer (pH 7.2–7.4) and block-stained in aqueous uranyl acetate [84]. However, microtubules were clearly apparent when the fixed eggs were post-treated with a tannic acid solution [185].

ties. This might reflect the transport of specific cytoplasmic constituents towards the dorsal yolk free cytoplasm (DYFC) [6, 10, 13, 84] by treadmilling, or microtubule associated proteins (MAPs) could mediate transient interactions of microtubules with other cell components, providing a way of transport for relatively large molecular complexes towards the animal-dorsal part of the uncleaved fertilized egg [82]. In the DYFC many rather long MTs were observed at NT 0.66 (fig. 2), but absent at NT 0.80.

In fertilized eggs the amount of polymerized tubulin in spermaster and wave front increased from NT 0.2 onwards and decreased after NT 0.6 when the natural break-down of spermaster rays starts; break-down of the thinner fibrils in the wave front started at NT 0.8 [82]. In prick-activated eggs a similar sphere-like MT-entity composed of thin tubulin fibrils developed only from post-pricking¹ 'NT' 0.4 onwards, radiating from a point slightly below the female pronucleus (not shown) and disappeared after NT 0.8. In such activated eggs either a normally latently present female centriole [108] is activated or the nucleus itself [93, 97] acts as MTOC. We occasionally observed a similar structure developing in the fertilized egg (not shown). Although it is much

¹ Eggs from the same batch were fertilized at the time that the others were pricked.

less dominant than the spermaster, we suggest that this MT-entity is involved in the movement of the central cytoplasm (CC), together with (part of) the germinal vesicle content, towards the dorsal side, to form the transient DYFC [6, 10, 13, 84], plate IA and fig. 2. Thus polymerization and depolymerization apparently need the same period of time, but the polymerization starts earlier in fertilized eggs than in prick-activated eggs [82, 82a, 112].

Transient modifications of the egg's cytoskeleton create cytoplasmic asymmetries

Through vitellogenesis, fertilization and cleavage divisions about 1% of the total amount of soluble proteins consists of free tubulin dimers and microtubules [117]. Intrinsic dynamic instabilities of microtubules, actin filaments and cytoskeleton-associated proteins cause cytoskeletal arrays to reorganize in response to internal and external cues [113–116; 38 for review]. Amount, status and distribution of the tubulin are correlated with the stage of development of the oocyte or embryo [37, 117, 117a].

Many relatively stable microtubules which did not label with antibodies against α -tyrosinated tubulin [82a] were observed in the penetration path of the male pronucleus (plate I, D), and in the vicinity of the centrosome. Posttranslational acetylation or detyrosination may stabilize (part of the) microtubules and thus generate a more constant cell architecture. This would need less energy and could act more efficiently than a system in which microtubule entities maintain a constant equilibrium between assembly and disassembly of microtubule subunits [82a, 118].

Microtubules drive the vegetal cortical rotation establishing antero-dorsal polarity

In 6 μ m histological sections of *Xenopus* eggs fixed in Bouin d'Hollande at NT 0.2, PAP staining revealed small patches of tubulin located immediately beneath the plasmalemma, which progressively spread, flattened (NT 0.4) and ultimately merged together into a continuous layer of tubulin (NT 0.6–0.8) directly beneath the plasmalemma (plate I, E and F) of the entire vegetal hemisphere [82]. After vinblastine incubation neither spermaster nor cortical array are present. The genesis of this cortical tubulin layer (which also contains γ -tubulin) inside and in immediate contact with the cell membrane of the vegetal hemisphere may foreshadow, and may provide a guide, for the formation of the transient vegetal cortical array of parallel microtubules involved in the ultimate determination of dorsal-ventral polarity [81, 110, 119–121].

The vegetal cortical array of parallel microtubules is the second main and independent microtubule entity [107] in the fertilized egg before first cleavage. It originates from a disordered array of microtubules [122] which

progressively transforms into a transient array of parallel microtubules, assumed to serve as tracks for rotation of the cortical cytoplasm around the more internal yolk mass, much like a railway line [110]. These microtubules finally cover the vegetal half of the egg and are oriented with their plus ends in the direction of the cortical rotation, i.e. ventro-dorsally. Shortly before and during the cortical rotation (NT 0.45–0.85) [120], non-astral microtubules of different lengths fuse with astral microtubules to form a dense network of radially organized cytoplasmic microtubules throughout the cytoplasm [75, 123]. Many of these microtubules also gradually merge with non-astral cytoplasmic microtubules [124], and become part of the band of parallel microtubules in the vegetal cortex [123]. They approach the cortex at an oblique angle and tend to continue in the same direction as the vegetal cortical array, i.e. with their plus ends away from the SEP towards the prospective dorsal side [123, 125, 126].

In normal development, at about NT = 0.5 (i.e. about halfway through the first cleavage cycle) the entire egg cortex rotates relative to the subcortical cytoplasm by ± 30 degrees about a horizontal axis in a direction away from gravity and in a plane coinciding with the future dorso-ventral plane of the embryo [110, 119–121, 123, 126]. A kinesine motor probably drives the rotation [125, 126], with a speed of 16 μ m/sec (fig. 3) [82a].

Through the first third of the first cell cycle, i.e. the period preceding the cortical rotation (NT 0.45–0.85), the formation of the cortical array in *Xenopus* eggs reveals a batch-dependent sensitivity to heavy water (D₂O). The cortical rotation can be manipulated by D₂O pulse treatments which seem to act by increasing the response of the egg to the cortical rotation [127].

Hyperdorso-anterior embryos and twins often form from eggs treated with 30–70% D₂O for a few minutes. Increasing concentrations of D₂O and prolonged exposure times gave rise to the formation of larger dorsal and more anterior structures, and reduced ventral and posterior ones. The vegetal half of the egg is most sensitive to the treatment [127], and although the direction of the cortical rotation is often opposite to normal, i.e. close to the SEP meridian, it always predicts the position of the future dorsal midline [110, 127]. Using the same concentrations and a 5 minute D₂O pulse treatment and careful washes between NT 0.16 and NT 0.3, we obtained embryos with *anterior duplications* (twinning) and *posterior reductions*. However, though the eggs are relatively insensitive to D₂O through the NT 0.3–NT 0.7 interval, towards the end of the cortical rotation period the eggs again become very sensitive to similar D₂O concentrations given as an identical (i.e. 5 min) pulse treatment [128]. In the latter case embryos with severely perturbed posterior regions and even twinned tails formed (not shown). In both cases about 30–40% of embryos were perturbed.

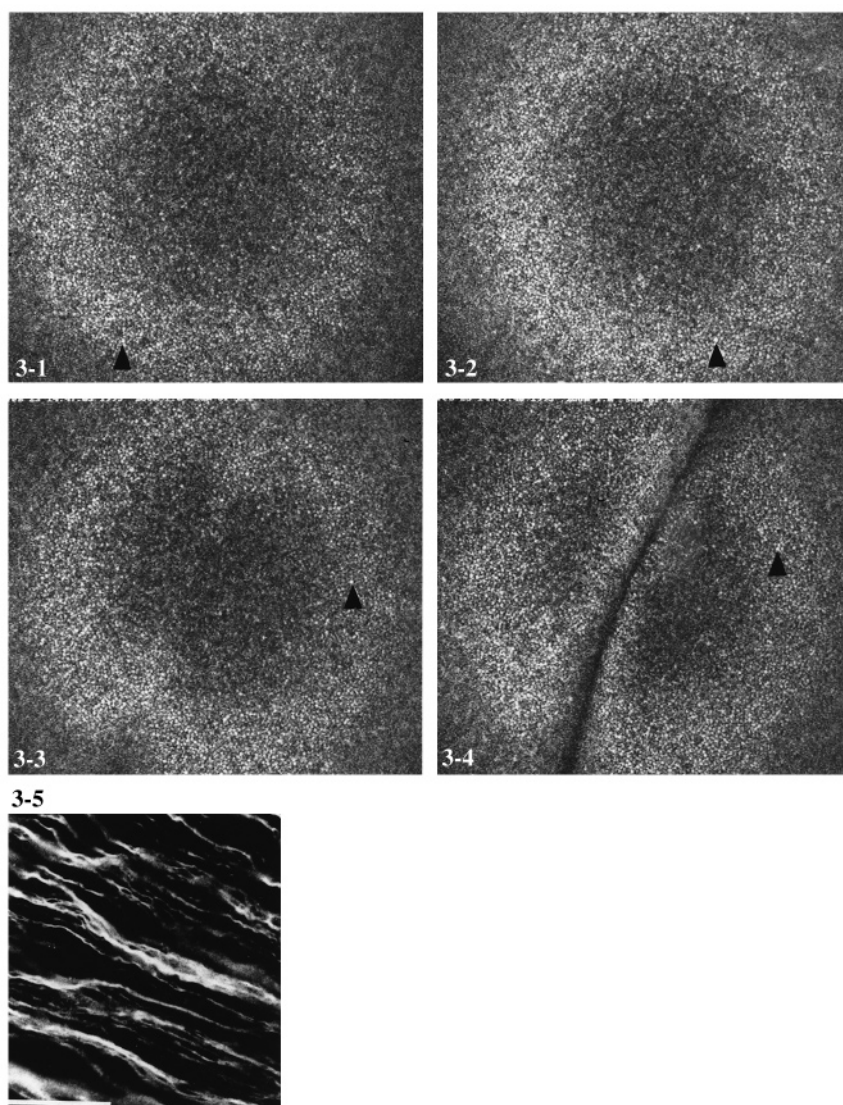


Figure 3. Visualization of the cortical rotation in live *Xenopus* egg. Movement of Trypan blue-labelled yolk granules in the vegetal hemisphere, in vivo visualized from below by Inverted-Confocal Laser Scanning Microscopy (I-CLSM) through rhodamine fluorescence [49, 50]. Eggs were not immobilized by gelatin, thus the vegetal cortical layer could freely rotate [96, 120]. Triangles in figure 3-1, 3-2, 3-3, 3-4 in sequence point to the same granule, which was video-registered during the cortical rotation, lasting from NT 0.47-NT 0.82, i.e. 31 min. Linear displacement was $301.44 \mu\text{m}$ i.e. about $0.16 \mu\text{m sec}^{-1}$; (based on theoretical calculations [120]: $0.17 \mu\text{m sec}^{-1}$; cf. ref. 96). (3-5) Bundles of microtubules in a fragment of vegetal cortex, revealed by immunofluorescence (refs 107 and 82a). Fixation: methanol at -20°C , post-fixed in acetone [110]. (Reprinted with permission from: Gerhart J. et al. (1986) Primary and Secondary Polarity of the Amphibian Oocyte and Egg. In: Gametogenesis and the Early Embryo, pp. 305-319, John Wiley & Sons, Inc., New York).

Grey crescent formation and the cortical rotation

The upper limit of the vegetal cortical array of parallel microtubules correlates well with the animalward shift of the limit of aggregated pigment granules in the animal cortex [13] at the prospective dorsal side of the embryo. The arc over which the cortical array shifts represents the grey crescent, visualized as a region of the egg cortex with dispersed pigment [6, 12 and refs therein], marking the future dorsal side of the egg. The cortical rotation [52, 120] is the principal cause of grey crescent formation, though some pigment contraction upon the SEP [13] occurs before the rotation starts [6]. The dorsal lip of the blastopore, the Spemann organizer [29], forms in

the amphibian embryo slightly vegetally from the equator on the meridian about 180° of arc away from the SEP. The SEP is more concise and therefore marks the D/V axis more accurately in experiments on axis formation than the grey crescent. The cortical rotation, as it is now generally called [1], is a crucial event for axis formation, in which microtubules are essential: all treatments perturbing microtubule formation and functioning interfere with the extent and direction of the global rotation as well as with axis formation [6, 12, 54, 119, 126]. As are the other cytoplasmic relocations, this global rotation about a horizontal axis perpendicular to the future dorso-ventral plane, is in a still unknown way

cued by the sperm. However, the sperm is *not required* for this polarization [50].

The visibility of the grey crescent depends on the pigmentation of the *Xenopus* eggs, i.e. on the female which produced them. Yolk platelets located adjacent to the moving cortical layer are drawn with it, forming the vitelline wall [12]. Prick-activated eggs also form a grey crescent at the same time as fertilized eggs would do, but its localization is unpredictable [6, 7, 12, 54] and independent of the prick point. In such eggs the direction of the vegetal cortical array is independent of the prick point, and the orientation of the cortical rotation unpredictable [119–121].

The sperm is not required for generation of the vegetal cortical array of microtubules

The vegetal parallel microtubule array can form without any interaction with the sperm centrosome or any other microtubule organizing centre in the animal half of the egg [49, 50]. Similar structures form in pieces of vegetal cortex from bisected eggs, isolated immediately after fertilization or artificial activation of the eggs [107].

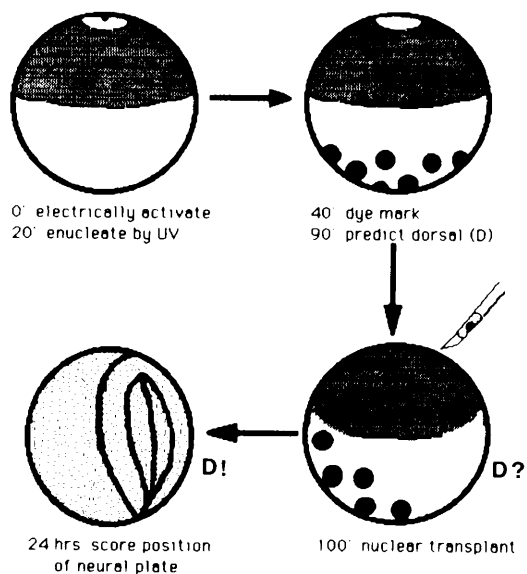


Figure 4. The sperm is not required for axis specification. Upon artificial activation by electric shock or needle puncture, and subsequent inactivation of maternal chromosomes with UV, unfertilized dejellied eggs (in which the cortex is immobilized by gelatin and the yolk can rotate with respect to the cortex) perform a yolk rotation similar to that in fertilized eggs, but along an unpredictable meridian. Such eggs continue to develop if they are provided with a diploid nucleus from a blastula. The position of the dorsal lip of the blastopore or the dorsal midline of the embryo can be scored, as neural groove of the neural plate at the meridian, predicted by the yolk rotation. The rotation of the subcortical cytoplasm of the egg in the first cell cycle was normal with respect to timing, extent, and effect on development. Apparently the egg does not require any sperm components to start yolk rotation and can form an anterior-dorsal axis when it is provided with a $2n$ nucleus after the cortical rotation. With permission after Gerhart et al. [50]; modified legend. (Reprinted with permission from: Gehart J. et al. (1986) Primary and Secondary Polarity of the Amphibian Oocyte and Egg. In: Gametogenesis and the Early Embryo, pp. 305–319, John Wiley & Sons, Inc., New York).

Upon artificial activation by electric shock or needle puncture, and subsequent inactivation of maternal chromosomes with UV, unfertilized dejellied eggs (in which the egg surface is immobilized through embedding in gelatin) do perform a yolk rotation with respect to the cortex similar to that in fertilized eggs, but along an unpredictable meridian [50]. This was visualized by labelling of the superficial layer of yolk. Such eggs continue to develop if they are provided with a diploid nucleus from a blastula. The position of the dorsal lip of the blastopore or the dorsal midline of the embryo can be scored, as neural groove of the neural plate at the meridian, predicted by the yolk rotation. The rotation of the subcortical cytoplasm of the egg in the first cell cycle was normal with respect to timing, extent, and effect on development despite the absence of the sperm (fig. 4). The egg apparently does not require any sperm components to start yolk rotation and can form an embryo with an anterior-dorsal axis when it is provided with a $2n$ nucleus after the cortical rotation.

In the darkly pigmented eggs of the anuran *Discoglossus pictus*, the grey crescent always shows up clearly at the future dorsal side of the egg. Cytoplasmic segregation starts during maturation and proceeds with the same developmental period as in *Xenopus*, also foreshadowing the future body axis, but in this species the sperm penetrates very near to the animal pole (fig. 9B) [51]. In different anuran amphibians sperm penetration initiates a polarized cytoplasmic segregation and cues the cortical rotation; in *Discoglossus* eggs the sperm does activate the egg, but it is unclear which cue governs the bilateral symmetrical cytoplasmic segregation started after sperm penetration. The cytological analysis strongly suggests that the grey crescent forms through rotation of the cortex [51] around the internal yolk mass at the same relative developmental time (NT) as in *Xenopus* eggs (cf. fig. 9, and legend). However, this has not yet been visualized in live eggs.

Developmental fate of distinct cells and the analysis of mesoderm induction. Factors involved in mesoderm induction are being identified with the aid of reliable dyes such as Texas red-lysine dextran (TRLDX), fluorescein-lysine dextran (FLDX), Lucifer Yellow, horse radish peroxidase (HRP) and specific molecular markers, accurately co-injected into the proper blastomere(s) at right developmental time(s).

Such analyses require accurate studies of cell lineages in the amphibian embryo. In *Xenopus laevis* in most of the cases the first cleavage furrow passes through the SEP [12, 54] but it does not always define the plane of bilateral symmetry, because the first cleavage plane and the embryonic axis are determined by different mechanisms [129, 130]. Since the early cleavage pattern in egg samples of particular females is variable, females used for this kind of experiments should be pre-selected.

Furthermore, when performing injection experiments or applying the animal cap assay in experiments on mesoderm induction [131, 131a] one should consider that pre-gastrular movements and epibolic extension of the animal cap cells [25, 26, 132] can change the positions of blastomeres and cause mixing of clones [132a]. Also the *time* of isolation as well as *size* of the explant can determine cell fate, e.g. the presence of some descendants of B₁ in a stage 8 cap may account for the ability of activin to induce dorsal mesoderm only from dorsal halves of the cap [131, 133, 134].

In various cell clones in *Rana pipiens* embryos at the 32-cell stage an extensive overlap of cell fates exists, but the overall spectrum of the origin of the various tissues from particular blastomeres was found to be quite similar to that in *Xenopus laevis* [135]. Existing interspecific variations are explained in terms of differential segregation of localized cytoplasmic components involved in cell determination during cleavage. However, in contrast to *Xenopus laevis* in which the mesoderm forms in the internal marginal zone [18], superficial cells in the early gastrula of *R. pipiens* contribute to mesodermal derivatives. In the urodelean *Pleurodeles* all mesodermal derivatives are formed from both superficial and deep cell layers [135].

Cortical rotation probably assists in the formation of the Nieuwkoop centre

The only distinct cytoplasmic localizations in the mature unfertilized egg are the germ plasm, located near the vegetal pole [14, 26], and a centrally located yolk-poor and cytoplasm-rich area (CC) [6, 10, 79]. A normal cortical rotation [1] is essential for normal development. It could function in localizing dorsal information to a particular area of the egg margin [95, 126, 136].

The spermaster initiates and directs the relocation of cytoplasmic components involved in dorso-ventral polarization of the egg, among them a shift of the CC towards a more dorsal and animal position (refs 6, 10, 13, 84 and plate I). The CC originates when the germinal vesicle breaks down and its content mixes with components in the mitochondria-rich region [78, 95, 137]. After some hours of in vitro maturation an area with a similar appearance was found at the basal side of the nucleus in oocytes from different amphibian species [78], suggesting that cytoplasmic segregation starts soon after resolution of the germinal vesicle. The period from full-grown oocyte to the mature unfertilized egg is characterized by significant changes in the cytoplasm, e.g. release of Vg1 RNA from the cortex and modifications in the cytoskeleton [3, 109].

When at NT 0.3 spermaster rays reach the egg centre [6], the CC starts shifting towards its most dorsal and animal position which is reached at NT 0.66, and from then on forms the DYFC [6, 10, 82, 84]. It is variable in

shape, has a diameter ca. 100–150 µm, and was further characterized by cytochemical methods and TEM as a highly metabolically active region, with up to 5 µm-long cytoplasmic cisternae, often oriented in the dorsal-ventral plane, large numbers of ribosomes, many mitochondria, some Golgi structures, many cytoplasmic vesicles and much glycogen [84]. The fraction of the total yolk-free area occupied by mitochondria was about three times that in the adjacent cytoplasm, and the number of cytoplasmic vesicles per unit area of cytoplasm was far larger than in the centre. In addition large numbers of microtubules (fig. 2) oriented towards the pronuclei could be visualized [6, 10]. Because of its stiffness, probably due to the presence of these MTs, the DYFC could be transplanted to another egg region or egg, but the results are not unambiguous. In egg rotation experiments the DYFC does not relocate while the dorso-ventral axis does change [6].

Selective fluorescent labelling of yolk granules revealed considerable movement in the deep cytoplasm of the animal hemisphere concomitant with the cortical rotation [96, 138]. Both the cytoplasmic rearrangements in the animal hemisphere initiated by the sperm and the cortical rotation, which starts in the vegetal half, assist through the first cell cycle in the differential distribution of mitochondria along the dorsal-ventral axis [70, 138, 139]. The dorsal side of the egg and prospective dorsal blastomeres become enriched in mitochondrial l-rRNAs, mitochondrial mRNAs and mitochondrial proteins, demonstrated by in situ hybridization [95]. These results confirm previous data, showing signs of enhanced metabolic activity [140; 4 for review] in dorsally located cells in the early *Xenopus* embryo. This could act in the determination of unique parts in the embryo, such as the Nieuwkoop centre [1] and/or the Spemann organizer [29]. Some cortical components, e.g. Vg 1 mRNA, localized around the vegetal pole in stage VI oocytes [2, 103, 145, 146], may be translocated closer to the place of origin of the Nieuwkoop centre by the cortical rotation, and interact with some other component(s) [95, 96, 136, 138] relocated through the deep cytoplasmic movements in the animal hemisphere.

Pre-cleavage cytoplasmic localizations may promote antero-dorsal development

Different experiments strongly suggest the presence of some dorsal cytoplasmic and/or cortical components involved in the determination of anterior/dorsal development in the *Xenopus* egg and/or embryo [4, 47].

Egg cortex transplantation experiments made Curtis [141, 142] propose that dorsally localized cortical determinants determine the dorso-ventral axis in the *Xenopus* embryo. Over a period of more than fifteen years his hypothesis prompted many interesting experiments. However, egg rotation and centrifugation experiments finally revealed that yolk shifts due to the slight tilting

of the recipient egg, needed for the attachment of the implanted piece of cortex and wound healing, rather than the transplantation of pieces of cortex, caused axis reversal and twin formation [12, 54, 143].

Among different kinds of analyses are antisense RNA injections into fertilized eggs as a test for the function of localized mRNAs [143a] egg rotation and centrifugation experiments [5, 6, 12, 52, 54, 66–68]; UV-irradiation of the vegetal hemisphere [1, 12, 54, 144–151 and 4 for review of classic literature]; manipulations of blastomeres [11, 16, 19, 20, 23, 41, 43, 46, 152, 153] including rotation of early animal blastomeres through 180 degrees which causes axis reversal, also through 180 degrees [154]; withdrawal of cytoplasm from different places in fertilized eggs, which supports the notion that factors indispensable for dorsal development are localized in the dorsal submarginal zone [44, 45, 155]; the vegetal-dorsal cells from the 8-cell embryo can form dorsal axial structures at a later stage [46]; bisection or ligation experiments before first cleavage confirm that cytoplasmic constituents responsible or indispensable for D-V axis specification are localized at the presumptive dorsal side of the egg before first cleavage [151]; all cytoplasmic factors required for the activation of muscle-specific genes are localized in the sub-equatorial region of the uncleaved *Xenopus* egg, mostly at the dorsal side [2, 151, 156].

UV-irradiation of the vegetal hemisphere of fertilized *Xenopus* eggs dose-dependently reduces or abolishes axis formation, producing embryos that lack dorsal and anterior structures [147]. Such embryos can be rescued by tilting the eggs over a few degrees with respect to gravity for a few minutes [149, 150]. It was assumed that the UV, which only penetrates superficially, destroys the array of parallel MT in the fertilized eggs [110, 120] and thus interferes with the mechanism of the cortical rotation which governs normal development. UV interferes for instance, with the dynamics of the localization of the germ plasm [150a].

Gravity, inducing a slight cytoplasmic shift, could mimic the cortical/cytoplasmic rotation [1, 6, 12, 67, 68, 119, 149, 150, 157] and rescue the embryo. However, eggs from ovarian oocytes which were artificially matured and UV-irradiated from below during prophase I also exhibited the dorsoanterior-deficient syndrome, but dorso-anterior development could not be rescued by tilting the eggs with respect to gravity. The UV-target in the artificially matured oocyte apparently differs from that in the fertilized egg and could be some dorsal determinant in the vegetal hemisphere [2, 144].

Gimlich and Gerhart [41, 158] were the first to show that UV-irradiated fertilized eggs can be rescued at the 32-cell stage by replacing *vegetal dorsal midline blastomeres* by the identical blastomeres from non-irradiated embryos, while twin embryos form when the two *vegetal ventral midline blastomeres* are interchanged with the

vegetal dorsal midline blastomeres from healthy 32-cell stage embryos. This suggests that dorsal blastomeres of early cleavage stages contain some important dorsal axis determinants. The authors assumed that the cortical rotation provides blastomeres with dorsal information to participate in embryonic axis formation [41] or to develop an axis autonomously [158, 159]. Injection of the *cytoplasm* of the identical *dorsal blastomeres* into the *ventral vegetal blastomeres* gives the same result as transplantation of entire blastomeres [136].

Furthermore animal dorsal midline cells of 16- and 32-cell stages, and maternal RNAs from 16-cell stage dorsal midline cells when injected into ventral blastomeres, induce a secondary dorsal axis and can restore the dorsal axis in UV-irradiated embryos [160]. The axis-inducing RNA molecules are located in the specific dorsal midline, animal blastomeres D 1.1 and D 1.2 of the 16-cell embryo (=fourth cleavage), whose descendants form most of the dorsal lip of the blastopore and during gastrulation the major part of the dorsal mesoderm.

The cytoplasm around the vegetal pole of a *Xenopus* egg, when injected into the *ventral vegetal* cells of a 16-cell recipient embryo, has the same axis-inducing activity as that of the *dorsal vegetal* cells of a 16-cell embryo [136]. It can induce a secondary axis before the cortical rotation occurs but, throughout the second half of the first cell cycle, its activity decreases gradually. Its reappearance in a presumptive dorsal equatorial region at the 2-through 16-cell stages is a prerequisite for normal development, suggesting that the determinant(s) responsible for this activity, predominantly located in the vegetal cortical cytoplasm [145], shift(s) from the vegetal pole to an equatorial region by or closely associated with the cortical rotation [161]. Such a shift does not occur in UV-irradiated embryos; while the cytoplasm around the vegetal pole of the fertilized egg keeps its dorsal axis-inducing activity, that in UV-irradiated oocytes is inactivated [145, 161].

Vg1 mRNA is synthesized in the oocyte and during vitellogenesis progressively localized to the vegetal cortical regions of *Xenopus* eggs and early embryos [40, 162]. Endogenous Vg1 accumulates as an unprocessed precursor and only very little mature Vg1 is formed. Injection of embryos with Vg1 mRNA results in the formation of high levels of Vg1 precursor, but no processed protein; it does not start mesoderm induction nor any other developmental event [102]. However, a soluble, biologically active mature Vg1, produced by expression of a hybrid activin β B-Vg1 molecule in *Xenopus* oocytes and injected at the 2-cell stage, can induce a complete body axis in animal cap explants [163]. This suggests that the active Vg1 fragment mimics the mesoderm inducing signal(s) normally released by the dorsal-vegetal blastomeres, which ultimately form endoderm and constitute the Nieuwkoop centre. This in its turn

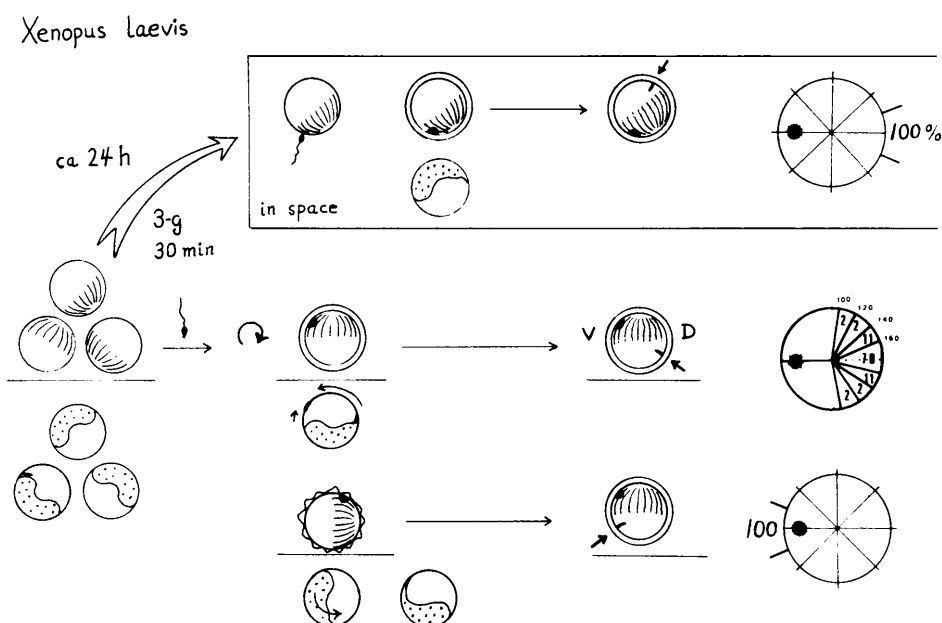


Figure 5. Design of rotation and microgravity experiments with *Xenopus laevis* eggs [12, 54]. Upper row: Under microgravity conditions, the A/V axis will remain in an arbitrary position. In all eggs, the blastopore is expected to develop either opposite the SEP or in a randomized position. Middle row: In normal development, the A/V axis in unfertilized eggs is in an arbitrary position with respect to gravity, but after rotation upon fertilization it becomes vertical. About 10 h later the blastopore forms opposite the SEP in about 70% of cases [12, 54]. Lower row: When a fertilized egg is put with its A/V axis horizontally and SEP-up, or in a centrifuge with the SEP in the centre of the rotor, the blastopore forms at the SEP side (cf. plate II: J and K).

could induce dorsal mesoderm, forming the Spemann organizer, which then governs the pattern of the embryonic axes [1, 164].

Deep cytoplasmic movements in the animal hemisphere of fertilized *Xenopus* eggs [6, 82, 96, 138] (also seen in the anuran *Discoglossus pictus* [51]) occur prior to and at the same time as the cortical rotation (fig. 9). The cortical rotation could direct the localized processing of the Vg1 precursor, forming the Nieuwkoop centre, and the proteolytic activation of the Vg1 could depend on a locally activated protease or restricted release of a cleavage site inhibitor [163], thus forming Vg1 protein at the dorsal side. The DYFC is a highly metabolically active region which contains many enzymes and mitochondria [6, 10, 84]. These components could be translocated towards the dorsal side by the deep cytoplasmic movements in the animal hemisphere, activating Vg1 and subsequently the Nieuwkoop centre.

This discussion favours an essential role of Vg1 as an endogenous factor acting in the formation of the Nieuwkoop centre and the subsequent dorso-ventral patterning of the mesoderm in the *Xenopus* embryo [2, 22, 36, 40, 101, 102, 145, 161, 163]. However, more recently, it has also been suggested that the cortical dorsal factor behaves more like a competence modifier, i.e. alters the response of cells to mesoderm inducers, than as a mesoderm inducer itself [146].

Egg rotation and centrifugation perturb normal axis formation, which suggested that gravity may play an essential role in embryonic pattern formation

In the fertilized *Xenopus* egg, pigment concentrates at the sperm entry point (SEP) and marks the egg meridian which foreshadows the prospective ventral side of the embryo in 70–80% of embryos; the blastopore forms at the meridian about 180° away from the SEP. This relation is thus not an absolute one, which suggests that additional factors are involved. However, the general body pattern of the embryo is established from then on [6, 12, 54] and the early recognizability of the orientation of the embryonic axes [13] enables us to manipulate axis formation.

In experimentally rotated fertilized eggs in which the cortex is immobilized, the superficial layer of the yolk shifts in relation to the cortex under the influence of gravity and centrifugal forces [5, 6, 12, 52, 54, 66]. The prospective dorso-ventral axis then forms in a position which is determined by the time of treatment and the angle and direction of the rotation [12, 54, 67, 68, 165]. The dorsal side develops at the meridian which was uppermost during the treatment [1, 4, 56, 59]. Thus, in such experiments, the cueing action of the sperm can be overruled by gravity or centrifugal forces (fig. 5), either through orienting the microtubules involved in the polarization, or by directly moving the cytoplasm without

involvement of microtubules [126, 157]. Our observations were made at 1g on eggs tipped over by 90° and kept immobilized by gelatin or Ficoll. Under these conditions only the peripheral layer of yolk rotated, the DYFC and more internal yolk materials did not relocate [6].

In contrast to Curtis's cortex transplantation experiments [141, 142] these egg rotation experiments suggested to us that neither the dorsal egg cortex nor the DYFC contain particulate dorsal determinants essential for axis formation [12, 54]. They also confirmed some classical findings [4 for review], and again strongly suggested that in normal development gravity is involved in the determination of the spatial structure of the amphibian embryo. Logically, this could only be tested by making an analysis of amphibian development under μ g conditions (fig. 5). The results of experiments performed in μ g during flights of space shuttles and sounding rockets showed that gravity is not required for axis formation.

Fertilization and development of *Xenopus laevis* eggs in real and simulated microgravity

During evolution living organisms on Earth were permanently subjected to gravity and developed special structures to perceive and to cope with this constantly acting natural force. In experiments the absence of gravity perturbs cell functions such as cell proliferation, adhesion, fusion and differentiation essential for normal embryonic development (for reviews, see refs 166–168).

Very different biological systems, e.g. bacteria [169, 170], yeast cells [170a], *Paramecium* [167], ovarian oocytes in *Drosophila*, *Artemia* [171] and human lymphocytes attached to microcarriers [172], cultured mammalian lung and pancreas rudiments [172a] show an increased mitotic rate; Sf9 cells [173] are insensitive to μ g, while the mitotic rate is reduced in free lymphocytes [167]; in A431 carcinoma cells [174] expression of the early genes *c-fos* and *c-jun*, both involved in cell proliferation, is reduced by about 50%. Thus μ g interferes with different regulatory mechanisms in mitotic signalling, to an extent depending on the nature of the regulatory mechanism and the cells involved. So different kinds of cancer cells are more or less sensitive to the μ g surroundings.

If microgravity shocks or longer periods of different gravity loads are perceived and in some way transferred in eggs or embryos, μ g could perturb normal development through for example perturbation of embryonic axis formation, as was suggested by some classical embryological experiments [6, 52, 55, 57, 58, 60; and 4 for review]. In sounding rocket experiments providing 6–7 minutes' μ g, the loss of gravity could act as a signal in developmental processes similar to the way that heat shocks can at particular times in development [64, 65, 175]. On the other hand *Rana pipiens* embryos at the 2-cell stage launched in the space shuttle were reported to develop normally [174a].

To test whether indeed μ g in some way interferes with normal development of the amphibian embryo, we made successful fertilization experiments (table 1, plate II and fig. 6) and found that fertilization in μ g initiated normal embryonic development.

Experimental procedures

Experiments on fertilization and early development of *Xenopus* eggs and embryos in microgravity (μ g) were performed during space shuttle flights launched from Kennedy Space Centre (Florida, USA), in Space Lab in the BIORACK: in 1985, D₁ [61]; in 1992, during IML-1, cf. fig. 6 and plate II: B, C, G-I [27, 28]; in 1994, during IML-2, cf. this publication, and De Mazière et al., in prep.; or aboard sounding rockets (SR) [65a for review], launched from ESRANGE, Kiruna (Sweden): in 1988, TEXUS-17, cf. plate II: A, B, figure 6 [106, 176]; in 1989, MASER-3, cf. plate II: A, B, D, E, F1 and F2 [64, 65, 175]; in 1993, MASER-6 [63], cf. plate II, A; figures 6 and 7; table 1. In most cases an identical experiment was simultaneously performed in a flying 1g control centrifuge, and two hours later on Earth. For these experiments we used only skin-marked *Xenopus* females [28, 61, 177], pre-selected at the Hubrecht Laboratory, Utrecht (NL), by performing fertilization tests every three or four months, at 0 and 24 h (stored at 10 °C) after stripping. The eggs were also individually selected for e.g. a regular maturation patch (i.e. equidistant from the equatorial pigment boundary) and for a regular general pigment pattern, before loading them into automated experiment containers (AECs; plate II B; fig. 7). Eight AECs were simultaneously flown in SRs, and six in Space Lab missions; similar numbers of AECs were activated on Earth. Manually operated flight module-type laboratory modules were used for testing of the experimental procedures.

Three to four weeks before arrival of the toads, we set up a small amphibian facility near the launching site, with a simple water pumping system, filtering the circulating tap water and maintaining the temperature at about 22 °C. The toads were flown in at ESRANGE (Kiruna, Sweden) or Hangar L at Kennedy Space Centre (KSC; Florida, USA) under very well controlled conditions, packed in insulated picnic boxes partly filled with wet foam cuttings [27, 28]. Special care was taken to avoid shocks and sudden temperature changes. About three weeks before launch 30 *Xenopus laevis* females and 40 males arrived and were immediately put separately into the aquaria. Seven to ten days later the frogs were well acclimatized and after hormonal stimulation under Hubrecht Laboratory standard conditions the females produced vital eggs.

On manned space shuttle missions one has to cope with relatively long periods of 'late access' (i.e. the interval between delivery of the experiment by the experimenter and launch of the vehicle) and, especially at the beginning

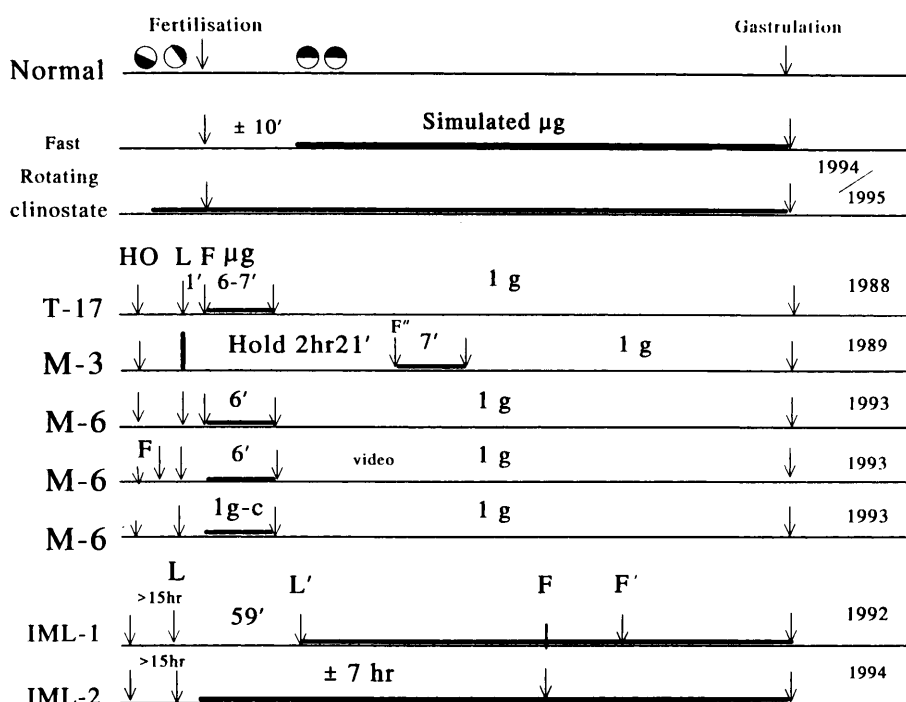


Figure 6. Summary of experiments with *Xenopus* eggs in simulated and actual microgravity. Upon sperm penetration the *Xenopus* egg rotates as a unit, turning its animal/vegetal axis upright, the heavy, yolky hemisphere down, the pigmented animal hemisphere up. Experiments on clinostates were started either after artificial fertilization on the bench, or by fertilization in the clinostate. The experiments in actual μg (± 6 min) on sounding rockets T-17, M-3, and M-6, were handed over (HO) relatively shortly (1–2 h) before launch (L), though e.g. weather conditions or malfunctioning of one of the experiments could cause a delay (cf. M-3) or abortion of the launch (as happened in the case of T-17, six days sequentially!). On SR M-6 an available video-recording facility was started shortly after fertilization on Earth, 5'30" min before launch; fertilization in a 1g centrifuge aboard, concomitantly with fertilization in microgravity, served as the proper control to confirm whether any developmental anomaly found was due to a real μg effect. Experiments in actual μg on an American space shuttle have to be delivered much earlier (i.e. in IML-1 and IML-2, about 15 h beforehand, which is expected to become still more in the future); also launch delays and abortions may occur. Fertilization in the shuttle could be performed only about 7 h after reaching μg .

of the missions, with astronauts who are too busy. Because of the limited viability of eggs and testes, and to reduce times and risks of handling during experiments, we designed automated hardware [61, 64, 178]. Moreover, in the various missions our experiment was one of the last to be handed over to ESA/NASA and one of the first that was activated in microgravity.

Fertilization in specially designed automated experiment containers (AECs). Prior to launch, testes freshly removed from hormonally activated males, and selected eggs obtained from hormonally stimulated preselected females, were loaded into the especially designed automated experiment containers (AECs; plate II B; fig. 7), which in the case of space shuttle missions were launched about 17 hours after stripping the eggs from the females; fertilization occurred only about 7 hours after launch, i.e. with a total delay of almost 24 hours, including time needed for preparation: stripping eggs from the females, egg selection, loading of the AECs, delivery to ESA/NASA personnel and shuttle loading, launching and hardware activation. To prevent these conditions ruining the experiment [179], over the years *Xenopus* females were selected which would reliably

produce sufficient numbers of eggs that survive perturbations of launching and can be fertilized with high efficiency even 24 hours after stripping and 'storage' under conditions of the experiment [61, 62].

The automated hardware (plate IIB; fig. 7) became a real advantage when flight opportunities on sounding rockets (SR) became regularly available (table 1 and fig. 6) [178]. Aboard SRs, vibration, accelerations and decelerations are much stronger but of shorter duration than those during shuttle flights. Furthermore, the much shorter period of 'late access' is very advantageous for short (i.e. 6–7 min) biological experiments in μg and the experimental materials can usually be returned to the experimenter's laboratory within about an hour. A 1g centrifuge and a video facility especially developed for the SR-MASER-6 mission functioned in flight very well.

As well as automated experiments on SR and space shuttle flights (table 1 and fig. 7), at different gravity loads we fertilized eggs in manually operated flight module-type laboratory modules, during 32 paraboles (g-spectrum: 0–1.8g) in a parabolic flight, and found axis formation more perturbed when the eggs were

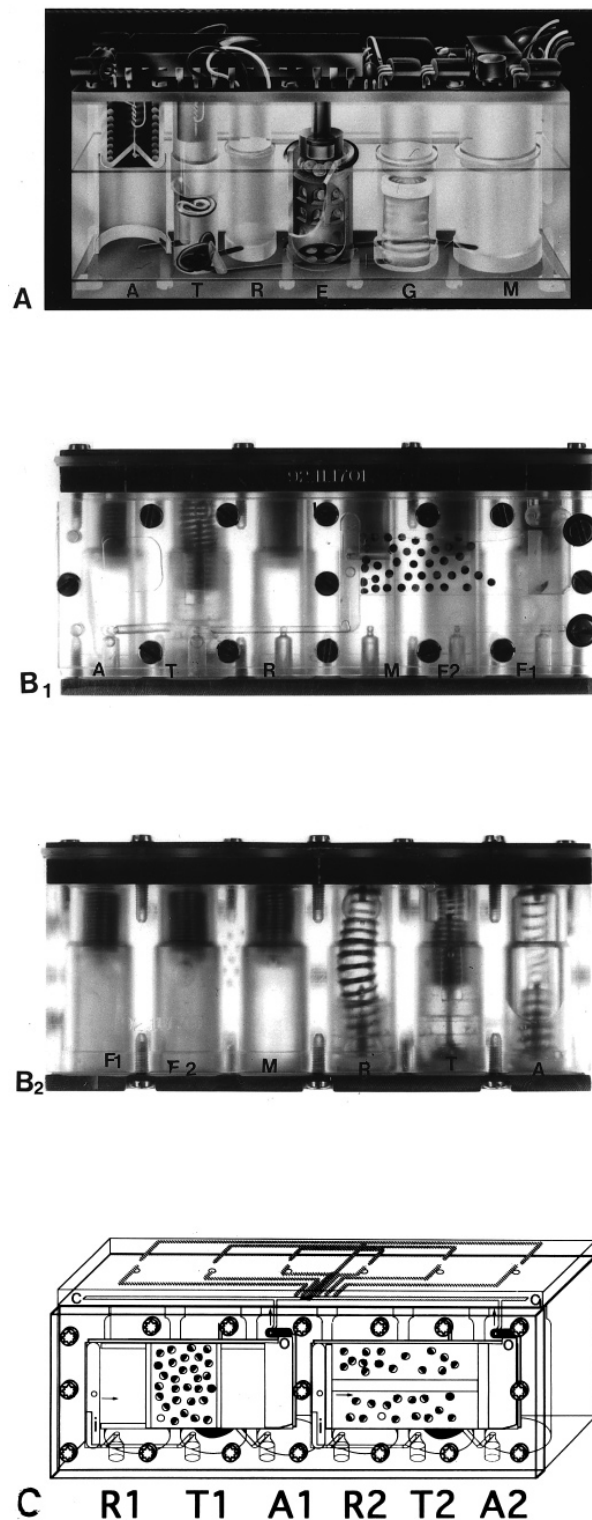


Figure 7. Fertilization of *Xenopus* eggs: various versions of the automated experiment container. (A) AEC used on SR TEXUS-17 and MASER-3, and space shuttle mission IML-1 [27, 28, 64]; c.f. plate II and 7ad. for experiment details. E: egg cylinder, T: testis cylinder, both with 100% MMR and eggs or testis; A and R: cylinders with 10% MMR, for fertilization. (B₁) AEC modified (mAEC) for the IML-2 space shuttle mission, providing improved circulation of fluids in the block, excellent visualization of two groups of embryos from different females for video-recording, in the now laterally positioned EGG compartment (E) (with two

sub-divisions), and the possibility of an extra wash or a post-fixation [63]. (B₂) mAEC, reversed side. Plungers, programmed for sequential activation to perform fertilization are down (T, A, R), the three additional ones providing washing and the two histological fixations (M, F₁, F₂), had not yet been activated [63]. (C) mAEC, used on the SR MASER-6, with two lateral EGG-compartments, and two sets of plungers, independently programmable for fertilization; twice as many eggs at a time could be fertilized. However, in this module fixation could not be performed [63]. N.B. In the drawing the left EGG compartment is adapted to the video-recording. The various inserts are interchangeable. Actual size of the AEC with electronics mounted on top: 79.5 × 19.0 × 40 mm (without electronics: height is 33.1 mm) [63, 178]. The AEC, used for SR experiments on TEXUS-17 and MASER-3 and the shuttle experiment during the IML-1 mission^a consists of a perspex cylinder block equipped with spring-activated pistons governed by a microprocessor for sequential operation, to start fluid transfers between the different compartments of the closed system [106, 175, 178]. Following the Hubrecht standard protocol *Xenopus* males and females were hormonally stimulated, males were killed for removal of the testes and eggs were 'stripped' from the females. Immediately after stripping eggs from the two best out of the (usually) four injected females were individually selected for a regular pigment pattern with special emphasis on the central position of the maturation spot. Within two h of stripping the AECs were loaded with salt solutions^b, histological fixative, a testis and selected eggs; in addition, after stripping the females for a second time after a two h interval, a second set of modules was prepared to be activated on Earth as a control, either in a CIS-module (in Kiruna) or in the Biorack (in Hangar L, KSC); control eggs were also fertilized in some laboratory modules and in dishes on the bench.

^a In SR experiments eight AECs were flown and electrically activated in an air-tight and temperature-controlled double-walled aluminium box. The temperature inside the experiment units was registered by an inbuilt temperature sensor, and in both the flight and the ground control experiment it rose by only 1 °C; during SR experiments the temperature was 17 or 20 °C; the pressure remained constant at 1 bar [106]. In the MASER-6 experiment the 0g box also contained a video recorder; as a control a second box was flown on a 1g centrifuge. Housekeeping signals were also registered during SR and shuttle experiments. In space shuttle experiments six AECs were individually inserted into type IE-Biorack containers and flown in the 22 °C incubator in the Biorack; two out of these were mounted on the control 1 g centrifuge, placed in the same incubator. The experiment sequence test (EST, 1990) had shown that under the conditions of the experiment, air circulation in incubator A (22 °C) was insufficient to let the AECs operate at about 22 °C. Therefore, for the IML-1 mission we determined a semi-automated experiment sequence, in which the astronauts were involved; for the IML-2 mission the AECs were equipped with low-power electronics.

^b Fifteen eggs from each of two different females and a testis were stored apart in the AECs, in 100% MMR, equilibrated to 230 mOsmol and pH 7.8, in shuttle experiments at 10 °C; fertilization was done at 22 °C in 10% MMR, embryo culture in 25% MMR. The glutaraldehyde-fixed gastrulae from IML-1 were de-jellied after retrieval, photographed from the animal and vegetal sides, and the images were stored in a live videodisk recording system (LVR). Thereafter, about 50% of the embryos were, through subsequent pigment bleaching, dehydration and clearing, prepared for analysis by confocal laser scanning microscopy (CLSM) as whole mounts. After CLSM, they were prepared for subsequent analysis by classical histology, the remaining ones for analysis by classical histology only [27, 28].

subjected to a greater number of parabolas before fertilization occurred (Mesland and Ubbels, unpublished observations).

Identical differences in gravity load, but now in low hyper-g (1.4–3.2g), were applied in the same rhythm for identical short durations in a specially designed centrifuge, accurately adjustable to low gravity values. This experiment was performed to find out whether any apparent μg effect was due to the difference in gravity load rather than to proper weightlessness. All samples developed normally, i.e. those on the special centrifuge as well as the 1g controls, fertilized just before and just after the two-hour lasting experiment in the centrifuge. Thus we assume that any developmental anomaly resulting from μg experiments is indeed due to weightlessness proper, and not to the fact that the embryo perceives a gravity load different from normal.

All our tests demonstrated that unfertilized *Xenopus* eggs from preselected females are resistant to the perturbations from SR launching, and to the less severe but 17-hours delayed shuttle launch perturbations, followed by another delay of 7 hours in μg conditions. In no case did these perturbations interfere with successful fertilization.

In microgravity sperm penetrate and induce axis formation in *Xenopus* eggs

In one of the first biological experiments on a sounding rocket (SR-TEXUS-17; May 2, 1988), about one minute after launching *Xenopus* eggs were fertilized successfully, and histologically fixed in flight within the period of actual microgravity, at 65, 138, 211, and 285 seconds post fertilization (p.f.) in four times two AECs (plate II B; fig. 7). Both SEM analysis (plate II, F₁ and F₂) after a critical point drying procedure and analysis of carefully prepared 6 μm serial histological sections (plate IID) showed that only one sperm per egg started to penetrate somewhere in the pigmented animal hemisphere. Thus the mechanism for monospermic fertilization is maintained under μg conditions [64, 106, 175].

Also for the first time, eggs of a vertebrate were successfully fertilized in μg . This was confirmed on SR MASER-3 in early 1989 [64, 65, 175]: within 1–3 minutes in flight in each of two containers sperm fused with eggs from two different females (female 1: 57% and 72% (64.5%), female 2, 75% and 83% (79%). Successful sperm penetration can be substantiated by incubating newly stripped eggs in a Hoechst solution during artificial fertilization (plate II, F₁ and F₂). In a pilot experiment in one of the eight AECs flown on SR MASER-3, *Xenopus* eggs from two different females were successfully fertilized in 25% MMR containing Hoechst 33258, after being soaked in the Hoechst solution (0.1 $\mu\text{g}/\text{ml}$ in 100% MMR) for nearly 6 hours (viz. during preparation, loading and the time elapsed till activation of the

AECs in flight), and then histologically fixed. Hoechst 33258 is a rapidly penetrating DNA-specific bisbenzimidazole fluorochrome which, even after fixation in 2.5% glutaraldehyde in 25% MMR, raised specific UV-fluorescence [175]. After flight, UV-microscopical analysis of whole mounts, and subsequent analysis of the same eggs by SEM, confirmed that sperm-egg fusion in microgravity led to real sperm penetration (plate IID) [64].

This experiment space-qualified the AEC, especially designed for the IML-1 space shuttle mission for flight under SR TEXUS-17, and SR MASER-3 conditions, and demonstrated the feasibility of biological experiments on such rockets despite strong perturbations during launch and reentry. From then on SR have been considered proper vehicles for short biological tests and in-flight functional tests of newly designed flight hardware for other missions [65a].

In a longer automated experiment on the American space shuttle 'Discovery' (IML-1 mission, January 22–30, 1992) we confirmed sperm penetration in μg , even after fertilization delayed for 24 hours, and found that in μg sperm penetration continues and starts embryonic development: in the automated modules gastrulae were fixed at the pre-programmed (=normal) time [27, 28].

This showed unequivocally for the very first time that *gravity is not required for axis formation!* Moreover in μg the *Xenopus* gastrulae developed with the same speed as at 1g.

Normal tadpoles retrieved from space after induction of ovulation, artificial fertilization and culture in μg

About half a year later (i.e. September 1992) these results were confirmed [69] on the SL-J space shuttle mission ($<10^{-3} \times \text{g}$). Thirty hours before launch four pre-selected female frogs, usually yielding high quality eggs, were put in a moist foam-lined container at 18 °C and sent into space. Eighteen hours into the mission the astronauts induced ovulation by injecting gonadotropic hormone and all frogs spawned at the proper time, which showed that the receptor-mediated uptake of the hormone under μg conditions occurs normally. The eggs were stripped by the astronauts, fertilized artificially and grown at 21 °C, either at zero gravity or in an onboard 1g centrifuge. Embryos were histologically fixed at different time intervals in flight, immediately after landing or when the 156 tadpoles that hatched in space, metamorphosed. Swimming tadpoles were video-registered in flight; others developed into seemingly normal larvae, metamorphosed normally and produced healthy Earth-born F₁ offspring, with an unimpaired reproductive function. An identical experiment was successfully performed simultaneously on Earth. Thus the anuran amphibian, *Xenopus laevis*, i.e. a vertebrate species, can ovulate in μg ; the eggs can be fertilized and

develop into normal free-swimming larvae in the seeming absence of gravity. In future, in space station experiments can thus be done with *Xenopus* eggs and embryos stripped onboard.

A most interesting experiment would be to launch some newly stripped *Xenopus* females for a stay in μg for at least three months, to find out whether, after induction of ovulation, stripping and artificial fertilization by the astronauts [cf. ref. 69], normal embryos develop in space. Ideally, some of these embryos should be kept there for another 18 months and subsequently spawned in the same way. If embryos continue to form normal axes, gravity does not play any determinative role in axis formation, either in ovarian oocytes or in subsequent embryonic development. This is the more interesting because a recent paper shows that off-axis orientation of oocytes during oogenesis could perturb an endogenous factor which normally causes provisional axial symmetry [70].

Embryos from SR and shuttle experiments consistently develop characteristic anomalies, but recover during gastrulation

In SL-J embryos at the 2-cell stage fixed in μg , the first meridian cleavage furrow was in the normal position but the mitotic asters in the two blastomeres were in a more equatorial position, thus shifted towards a more vegetal latitude [69] as previously described for embryos which developed during clinostate rotation [67, 68, 165, 180]. If the more vegetal position of the two nuclei remained so through the third cleavage, the (horizontal) third cleavage plane would indeed form at a more vegetal latitude [69], enlarging the size of the animal blastomeres. This could explain why in μg , gastrulae developed with blastopores at a slightly more vegetal latitude, and thicker blastocoel roofs occurred in μg blastulae and early gastrulae retrieved from the IML-1 [27, 28] and SL-J shuttle missions: 4 cell layers in μg , compared to 2–3 layers in 1g [69]. Unfortunately for technical reasons both groups (Ubbels et al. [27, 28] and Black (pers. comm.)) failed to fix embryos at third cleavage in actual μg , but larger animal blastomeres formed in clinostate experiments (cf. this study and refs 67, 68, 165, 180). Alternatively, in μg thicker blastocoel roofs could originate from a *reduced* radial interdigitation or intercalation of cells, processes which in 1g conditions drive the epibolic extension of the surface layer of the blastula [25, 26, 132]. This, however, is not logical since in the SL-J experiment the blastopores were slightly shifted to the vegetal pole. In all cases 1g control embryos developed normal blastocoel roofs. Similar to embryos in clinostate experiments [67, 68], the SL-J embryos recovered during gastrulation and developed normally, although they remained in μg .

A microgravity shock during fertilization and initiation of development perturbs formation of the blastocoel, but does not interfere with axis formation

In a pilot experiment during the SR MASER-3 mission, embryos fertilized in μg , but not histologically fixed survived reentry: they developed into seemingly normal gastrulae though, depending on the egg samples, they either died during neurulation or developed an abnormal axis (e.g. splitting or duplication of the notochord), probably due to abnormal gastrulation [64, 65, 175]. This was taken to suggest that a μg shock could interfere with axis formation.

During the SR MASER-6 flight the proper control, viz. a 1g centrifuge, could be operated on the rocket for the first time. In this experiment fertilizations were performed simultaneously in μg and in 1g conditions (rates: $\geq 80\%$), so that flight perturbations apart from the varying g-loads were identical for all egg samples. After retrieval the eggs were carefully grown on Earth and fixed at different times; 1g controls were also obtained by activating a similar set of modified AECs (m AECs) (fig. 7, B, C) on Earth. The larvae from all egg samples developed normal axes [63]. Thus, axis formation and subsequent development are normal, when automated fertilization and initiation of development take place in the relatively short period of actual μg during a SR-flight. We assume that the perturbed axis formation on SR MASER-3 [64, 65, 175] was due to using the different launcher or resulted from inherent properties of the egg samples, produced by different females.

The cortical contraction [6, 104], one of the earliest fertilization phenomena, was analysed by video-recording of newly fertilized eggs in flight and on Earth during the SR MASER-6 flight. After fertilization at 5 min 30 sec before launch, the contraction started in flight at 585 sec ± 10 sec (average \pm SD for 3 eggs), on Earth at 679 sec ± 19 sec p.f. (average \pm SD for 5 eggs). Thus in this experiment the cortical contraction initiated about 90 sec earlier in microgravity than on Earth, suggesting an acceleration of processes concerned with the contraction which had already started on Earth. In both groups sperm and eggs fused on Earth, and the contraction started only a few minutes thereafter. It is unlikely that the time differences found are due to differences in the speed of sperm-egg fusion. However, the flying container had been submitted to launch accelerations during sperm penetration for less than a minute, and we do not know whether such short perturbations are perceived by sperm and egg.

On Earth the entire process of contraction and relaxation takes about 12 minutes. In future this experiment should therefore be repeated and extended so that a larger number of eggs can be recorded simultaneously, preferably in a longer flight (e.g. on MAXUS, which provides about 15 minutes of μg), so that video-recording can

be started in μg immediately after fertilization, also in μg .

In histological sections taken parallel (to and) through the A/V axis in the animal pole region of blastulae grown on Earth after fertilization in μg on SR MASER-6, the A/V axis tended to pass more cells than in similar sections of 1g blastulae from eggs simultaneously fertilized in the flying 1g centrifuge, though not in a significant

number. Although these blastulae were fixed at a relatively early stage, this could suggest that thicker blastocoel roofs develop when the embryo experiences only 6 minutes of μg during fertilization and initiation of development.

An additional aspect of blastocoel formation after fertilization in μg on SR MASER-6 was that the floor of the blastocoel formed significantly closer to the vegetal pole than in embryos from eggs simultaneously fertilized in the onboard 1g centrifuge [63]. The mean ratios of the distance between the blastocoel floor and the vegetal pole, to the total height of the blastula, were (\pm SD): 0.463 ± 0.013 ($n = 4$) and 0.513 ± 0.012 ($n = 4$) ($0.02 < P < 0.05$), for embryos after fertilization in μg or 1g respectively.

These morphological aberrations were consistently found but, as in the SL-J shuttle experiment [69], did not perturb subsequent development. Gastrulae grown on Earth from eggs fertilized in μg , and simultaneously in the flying 1g centrifuge or on Earth, were analyzed by in situ hybridization; the *Xbra* gene was expressed in the early gastrula (stage 10–10 $\frac{1}{2}$) at normal place and time. Normal stage 22 and stage 41 larvae were obtained in all cases.

In μg *Xenopus* eggs perform normal numbers of synchronous egg cleavages

In *Xenopus* eggs the first ten cleavages are synchronous, and the newly fertilized *Xenopus* egg thus seemed an appropriate system to study the influence of μg on the duration of the cell cycle in a vertebrate. In an experiment performed during the IML-2 space shuttle mission (July 8–23, 1994; table 1, fig. 6) in μg and at 1g, *Xenopus* eggs were fertilized and fixed in m-AECs after fertilization and development for 200 min at 22 °C, i.e. at 1g about the time of the eighth cleavage. A hardware failure meant we harvested only a small number of blastulae.

These *Xenopus* embryos were prepared as whole mounts [181], stained with a specific fluorescent DNA stain, TO-PRO-3, a cyanine dye [182]. In both experimental groups the number of blastomeres at 200 min p.f. (i.e. under the experimental conditions applied, the time of the eighth cleavage at 1g) was determined by counting nuclei in optical serial sections, recorded by CLSM, every 15 μm . The total number of nuclei was not

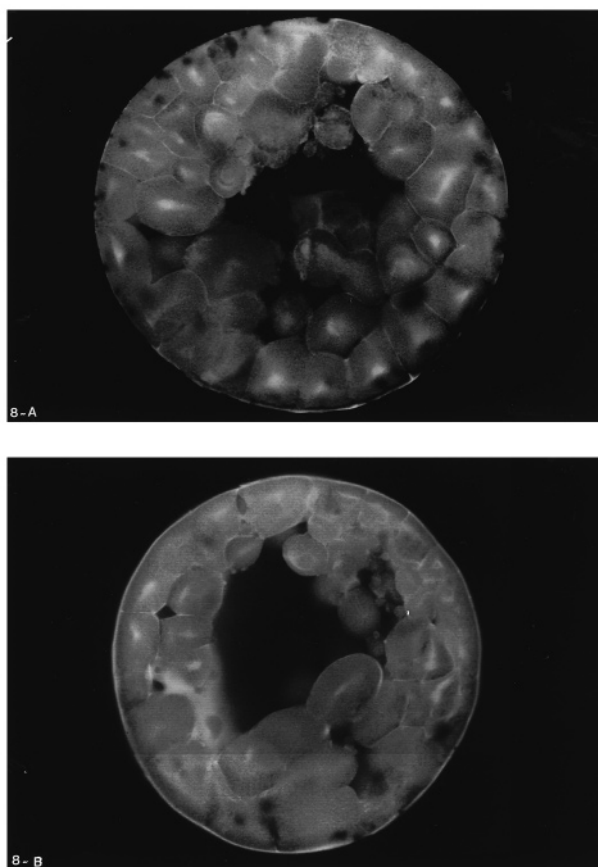


Figure 8. Blastocoel volumes. CLSM-pictures of *Xenopus laevis* blastulae: automated fertilization and fixation, during the IML-2 space shuttle mission. (A) in μg , and (B) at 1g. The volumes of the blastocoels were determined using CLSM software, by measurement and summation of surface areas occupied by the blastocoel in 15 μm thick serial optical sections. The blastocoel is significantly ($P < 0.05$) smaller in the μg embryos than in the 1g embryos (mean \pm SEM) 22 ± 6 nl ($n = 7$), versus 36 ± 4 nl ($n = 9$).

significantly different in μg and 1g embryos: (mean \pm SD) 333 ± 28 ($n = 6$) and 346 ± 18 ($n = 6$), respectively (Wilcoxon 2-sample test) [De Mazière et al., in prep.]. Thus the division tempo of these *Xenopus* blastulae during the early cleavages in actual μg was similar to that at 1g.

Xenopus embryos develop smaller blastocoels in actual and simulated μg

Several fixed gastrulae from the automated IML-1 shuttle experiment had irregular and severely reduced blastocoels, and in some embryos the blastocoel was even absent [27, 28]. In about half of the μg embryos from the IML-2 mission the blastocoel again had an irregular shape and was significantly smaller than in the 1g control sample (fig. 8).

Using CLSM software the blastocoel volumes were determined by measurement and summation of the surface areas occupied by the blastocoel in serial CLSM optical sections in:

Table 2. Blastocoel volume (nl).

Experiment	Embryos	
	1g control (mean ± SEM)	in actual/or simulated µg (mean ± SEM)
1) IML-2 24 h delay	(36 ± 4) nl (n = 9)	(22 ± 6) nl (n = 7)
2) a. Newly laid (0.01 < p < 0.02).	(33.3 ± 2.2) nl (n = 12)	(24.8 ± 2.4) nl (n = 11)
2) b. 24h delay p = 0.01	(32 ± 3) nl (n = 5)	(7.0 ± 3) nl (n = 5)

1) embryos retrieved from the IML-2 mission;
2) embryos from newly stripped eggs and eggs from the same *Xenopus* females but after 24 hours, storage at 10 °C, in both cases fertilized, and grown in a fast-rotating (60 rpm) clinostate (table 2 and fig. 8), and fixed at the eighth cleavage.

The volume (in nl) of the blastocoels in *Xenopus* blastulae retrieved from the IML-2 space shuttle mission was significantly smaller than those in the 1g control: (mean ± SEM) 22 ± 6 (n = 7) versus 36 ± 4 (n = 9). All embryos were from the same egg sample and fertilized with a 24 hour delay; [table 2, De Mazière et al., in prep.].

The volume of the blastocoel in blastulae from newly stripped eggs fertilized in the fast rotating (60 rpm) clinostate tubes was significantly smaller than those fertilized in the non-rotating tubes at 1g, though the difference between the two groups was less than in embryos from eggs stored for 24 hours (table 2). There is thus a small but significant effect of simulated µg on blastocoel formation, even in newly fertilized eggs. Delayed fertilization did apparently enhance the sensitivity of the embryos to the µg conditions.

There was no difference in the total volume of embryos from the sample after either fresh or delayed fertilization. The reduction in size of the blastocoel in the IML-2 embryos retrieved from microgravity is mainly due to the 24 hour delayed fertilization on the shuttle. In gastrulae fixed in flight during the SL-J experiment there was no significant difference in the volume of the blastocoel between the µg and 1g embryos (S. D. Black, personal communication).

Table 3. Clinostate experiments.

Experiment	1g control (mean ± SEM)	In simulated µg (mean ± SEM)
1) Thickness	152 ± 6 µm (n = 6)	204 ± 20 µm (n = 11)
2) Nuclei (n) Top segment	46 ± 6 (n = 6)	48 ± 4 (n = 11)
3) Nuclei (n) Whole embryo	340 ± 35 (n = 6)	320 ± 20 (n = 11)

- (1) Thickness of blastocoel roof (in µm).
(2) Number of nuclei in top segment of blastocoel roof.
(3) Number of nuclei in the whole embryo.

The results of experiments in actual µg are in good agreement with those in the fast rotating clinostat (table 2). Because of the limited numbers of IML-2 embryos, we performed additional experiments with eggs from different egg samples, in the fast-rotating clinostate (table 3) and measured the thickness of the blastocoel roof in blastulae fixed at the eighth cleavage. As in embryos grown from eggs fertilized during the SR MASER-6, IML-1 and SL-J missions, and compared to the Earth-based controls, the roof was thicker (cf. table 3: 1), but since the number of nuclei was similar in an identically sized top segment (table 3, 2), as well as in the whole control embryo (table 3: 3), in the roof of the blastocoels the cells were indeed probably bigger [69] than in the static tubes and the earth controls, due to a vegetal shift of the third cleavage plane (cf. De Mazière et al., in prep.), after fertilization and development in simulated [67, 68, 180] or actual [69] microgravity.

In normal development the blastocoel forms progressively by fusion of intercellular spaces in between the increasing number of blastomeres [25, 26]. The osmolarity of the blastocoel fluid is 220 mOsm and water accumulates in the blastocoel, probably due to an osmotic effect. The tight junctions between the surface cells and ion impermeability of the original egg membrane may prevent loss of ions to the outer medium, while the inner membranes are actively pumping ions. This could direct water movements through the semipermeable outer surface of the embryo [4]. New membrane formation along with the cleavage divisions will accelerate ion pumping [183]. The size of the blastocoel may thus be controlled by water exchange [4], and µg conditions in their turn could perturb these processes.

Blastocoel formation is perturbed after fertilization in simulated [this study; 67, 68] or actual [27, 28, 63–65, 69] µg, but from about stage 9 onwards the embryo recovers and develops normally [63, 67–69]. The abnormal blastocoel formation in simulated or actual µg does not apparently interfere with mesoderm induction, nor does pricking of the roof of the blastocoel and the subsequent reduction of its volume.

Four animal blastomeres isolated at the eight-cell stage can differentiate into dorsal mesodermal derivatives:

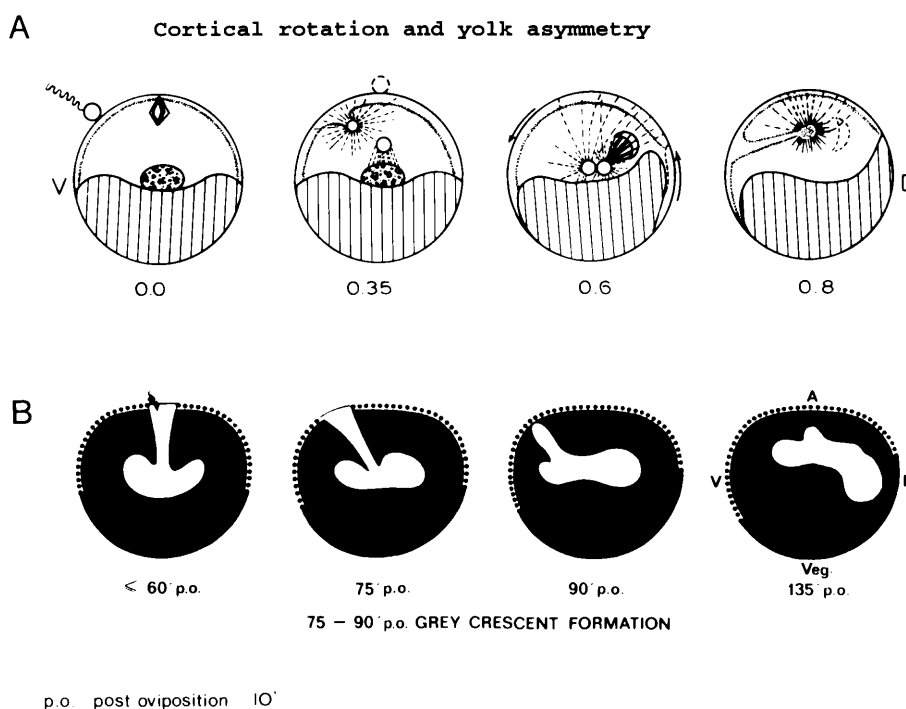


Figure 9. Deep cytoplasmic movements in the animal hemisphere and the cortical rotation symmetrize the *Xenopus* egg before first cleavage. (A) (modified after fig. 13 in ref. 6). The progressively expanding spermaster causes shifts of animal cytoplasmic materials, while the haploid female pronucleus, occasionally observed developing a tiny aster, moves centrally after extrusion of the second polar body. The pronuclei then lie together in the centre about NT 0.45, but progressively shift slightly dorsally, together with the central cytoplasm; meanwhile a cortical array of parallel microtubules drives the rotation of the cortical cytoplasm around the more internal yolk mass. Thus, in contrast our interpretation of the observations described in ref. [6], yolk shifts in the vegetal half are governed by a cortical rotation (NT 0.47–NT 0.82), and not by an asymmetrical cortical contraction. (B) In the egg of *Discoglossus pictus* the sperm always enters very near to the animal pole, and in the same developmental NT as in the *Xenopus* egg, initiates symmetrization in the pre-cleavage period, by cortical rotation [51]. Further analysis could reveal involvement of deep cytoplasmic movements (A).

developmental determinants distributed in distinct gradients during early cleavages, together with factors pre-localized in the marginal zone, could determine mesoderm formation by spatial and temporal activation of certain genes [152]. The suggestion that the developmental potential of such isolated animal quartets is gravity-dependent and results in gravity-dependent differential morphogenesis and gene regulation [180] is in conflict with the observation that embryos develop normally in microgravity [27, 28, 63, 69].

Concluding remarks

Provisional axial symmetry of full-grown *Xenopus* oocytes is broken during maturation

In our 1983 publication [6, p. 33] we wrote: '... the presence of the sperm and a microtubule array is essential for normal cytoplasmic segregation: obviously structuring of the cytoskeleton under influence of the sperm (most probably of its centriole), is essential for the establishment of the dorso-ventral axis and for normal development of the embryo upon egg activation'. Around NT 0.6, eggs are most sensitive to hydrostatic pressure or cold (treatments by which microtubules are broken down), and become radialized when high doses

are applied [1, 150]. At NT 0.6, the spermaster is maximally developed and we assumed that this is the reason that such treatments interfere with normal development, considering the spermaster to be the probable target of such perturbations [6]. However soon after this, J.-P. Vincent, repeating and extending AnceI and Vintemberger's impressive experiments, demonstrated that at about NT 0.6, during grey crescent formation, the external layer of the yolk moves with respect to the vegetal cortex when the latter is immobilized [120]. As in *Rana fusca* [52] and *Discoglossus pictus* [51], in normal development the entire egg cortex rotates relative to the subcortical cytoplasm by around 30 degrees about a horizontal axis, in a direction away from the SEP and gravity (fig. 9), in a plane coinciding with the future dorso-ventral plane of the embryo, and in some way cued by the sperm [1, 110, 119–121, 123, 126]. Thus in *Xenopus* too the grey crescent forms by rotation of the vegetal cortex and not by contraction [6, 13] of the pigment cap. The superficially located, vegetal array of parallel microtubules [110, 119–121] drives the cortical rotation and it is readily broken down by UV-irradiation from below [1, 150].

The grey crescent only actually forms opposite the SEP in about 70–80% of cases [12, 54, cf. table 2 in ref. 6],

suggesting the involvement of (an) additional factor(s). Upon prick- or electrical activation and subsequent enucleation by UV, the egg does form a grey crescent at the proper time but its location is now unpredictable. The vegetal cortical array of microtubules also forms, and as demonstrated in the Gerhart et al. experiment [49, 50], after introduction of a diploid nucleus from a blastula the neural groove forms at the meridian predicted by the yolk rotation, fig. 4 and [49, 50]. Thus neither egg nor sperm nucleus is uniquely required for the symmetrization of the mature egg.

In another anuran species *Discoglossus pictus* (fig. 9), as in *Xenopus laevis*, the fertilizing sperm initiates a cytoplasmic segregation and cortical rotation, and symmetrizes the fertilized egg in the identical relative developmental time span. However, in contrast to *Xenopus*, in the egg of *Discoglossus* the sperm always enters very close to the animal pole [51] and it is not likely that the asymmetry of the cortical rotation is due to the sperm penetration.

Gravity is not required for symmetrization

After fertilization of *Xenopus* eggs under microgravity conditions axis formation is normal [27, 28 and plate II] and normal tadpoles develop in the near-weightless conditions [69]. The cortical rotation is not driven by gravity, as suggested by [52], and the cytoplasmic rearrangements required for normal development do not need the gravity vector. Although blastocoel formation is perturbed under μg conditions [27, 28, 63; this review], from about stage 9 onwards the embryos recover and develop normally [69]. Thus microgravity does not interfere with mesoderm induction.

We suggest that the axial symmetry of the mature unfertilized anuran egg is provisional, and that asymmetry originates shortly after germinal vesicle breakdown when the nuclear content mixes with the materials of the CC and part of the Balbiani body, possibly including the oocyte's centrosome. Unequal distribution of these components among the yolk and formation of cytoplasmic localization(s) may cause provisional cytoplasmic asymmetry [95, 136, 139].

Afterword

In 1949 Pieter Nieuwkoop initiated the production of a Normal Table of the development of the South African toad, *Xenopus laevis*. In South Africa Job Faber collected the toads which became the nucleus from which the present *Xenopus* colony in the Hubrecht Laboratory is descended. Over the years many animals were sent to many different laboratories in different countries. The Normal table project was performed in collaboration with the staff of the Hubrecht Laboratory, university students and young scientists from abroad who tempo-

rarily worked as guests at the Hubrecht Laboratory. The first edition of the 'Normal Table of *Xenopus laevis* (Daudin)' by Pieter D. Nieuwkoop and Job Faber appeared in 1956, a second edition in 1967 with a first reprint in 1975. The recent reprint (Garland Publ., Inc. New York and London, 1994) of the *Xenopus laevis* Normal Table in its original form most clearly demonstrates current interest in *Xenopus* development and the need for this basic information.

When initiating the Normal Table project Nieuwkoop and Faber wrote in the 'General Introduction': '... the development of *Xenopus laevis* is quite interesting from a descriptive and comparative as well as from an experimental embryological point of view. Preliminary experiments demonstrated that the egg of *Xenopus laevis*, notwithstanding its very rapid development, is quite suitable for experimental work. Since the number of anuran species for which this is true is very restricted, a good basic knowledge of the normal development of this species seems to open new perspectives for experimental analysis in this group of vertebrates'. These days developmental biologists benefit much from the authors' foresight regarding the experimental possibilities offered by this species. Among them is the present author, who takes this opportunity to express her gratitude to both of the authors, most grateful for their continuous support and interest, being privileged to have worked with them in the Hubrecht Laboratory for many years!

Acknowledgements. We gratefully acknowledge financial support by the Netherlands Organization for Scientific Research (NWO) through the Space Research Organisation Netherlands (SRON/MG-013; MG-035), and by the Netherlands Academy of Arts and Sciences (KNAW), ESA and NASA. Thanks are due to the amphibian facility for careful frog culture; to Pieter Nieuwkoop and Tony Durston (the Hubrecht Laboratory), John Gerhart (U.C. Berkeley, USA), Steven Black (Reed College, Portland, Oregon, USA), Jirka Paleček and colleagues (Charles University, Prague, CR), for reading the manuscript and/or discussions; Oeke Kruijthof for library assistance, Wim Hage (CLSM) and the photographic department for preparing the illustrations, and Susann Maas for assistance in preparing the manuscript. Special thanks are also due to my crew members during different space missions, especially: Ann De Mazière, Jenny Narraway, Juan Gonzalez-Jurado, Mark Reijnen and Hans van Soest. Two Dutch companies, C.C.M. (Centre for Construction and Mechatronica, Nuenen) and F.S.S. (Fokker, Space and Systems, Leiden), developed the hardware and lent mission support.

- 1 Gerhart J. C., Danilchik M. V., Doniach T., Roberts S., Rowning B. and Stewart R. (1989) Cortical rotation of the *Xenopus* egg: Consequences for the anteroposterior pattern of embryonic dorsal development. *Development* **107**: Suppl. 37–51
- 2 Elinson R. P. and Holowacz T. (1995) Specifying the dorsoanterior axis in frogs: 70 years since Spemann and Mangold. *Curr. Top. Dev. Biol.* **30**: 253–285
- 3 Gard D. L. (1995) Axis formation during amphibian oogenesis: Reevaluating the role of the cytoskeleton. *Curr. Top. Dev. Biol.* **30**: 215–252
- 4 Gerhart J. C. (1980) Mechanisms regulating pattern formation in the amphibian egg and early embryo. In: *Molecular Organization and Cell function: Biological Regulation and Development*, vol. 2, pp. 133–316, Goldberger R. F. (ed.), Plenum Press, New York

- 5 Black S. D. (1989) A step in embryonic axis specification in *Xenopus laevis* is simulated by cytoplasmic displacements elicited by gravity and centrifugal force. *Adv. Space Res.* **9**: (11)159–(11)168
- 6 Ubbels G. A., Hara K., Koster C. H. and Kirschner M. W. (1983) Evidence for a functional role of the cytoskeleton in determination of the dorsoventral axis in *Xenopus laevis* eggs. *J. Embryol. Exp. Morph.* **77**: 15–37
- 7 Manes M. E. and Barbieri F. D. (1976) Symmetrization in the amphibian egg by disrupted sperm cells. *Dev. Biol.* **53**: 138–141
- 8 Manes M. E. and Barbieri F. D. (1977) On the possibility of spermaster involvement in dorso-ventral polarization and pronuclear migration in the amphibian egg. *J. Embryol. Exp. Morphol.* **40**: 187–197
- 9 Stewart-Savage J. and Grey R. D. (1982) The temporal and spatial relationships between cortical contraction, sperm trail formation and pronuclear migration in fertilized *Xenopus* eggs. *Roux's Arch. Dev. Biol.* **191**: 241–245
- 10 Ubbels G. (1977) A. Symmetrization of the fertilized egg of *Xenopus laevis* (studied by cytological, cytochemical and ultrastructural methods). *Symp. L. Gallien. Mém. Soc. Zool. France*, **41**: 103–115
- 11 Nieuwkoop P. D. (1969) The formation of the mesoderm in urodelean amphibians I. Induction by the endoderm. *Roux. Arch. Entwicklungsmech. Org.* **162**: 341–373
- 12 Gerhart J., Ubbels G., Black S., Hara K. and Kirschner M. (1981) A reinvestigation of the role of the grey crescent in axis formation in *Xenopus laevis*. *Nature* **292**: 511–516
- 13 Paleček J., Ubbels G. A. and Rzehak K. (1978) Changes of the external and internal pigment pattern upon fertilization in the egg of *Xenopus laevis*. *J. Embryol. Exp. Morphol.* **45**: 203–214
- 14 Czolowska R. (1969) Observations of the origin of the 'germinal cytoplasm' in *Xenopus laevis*. *J. Embryol. Exp. Morphol.* **22**: 229–251
- 15 Nieuwkoop P. D. and Sutasurja L. A. (1979) Primordial Germ Cells in the Chordates. Cambridge University Press, London
- 16 Nieuwkoop P. D. (1969) The origin of the dorso-ventral polarity of the mesoderm. *Roux. Arch. Entw. Org.* **163**: 298–315
- 17 Nieuwkoop P. D. (1973) The 'organization centre' of the amphibian embryo: its origin, spatial organization and morphogenetic action. *Adv. Morphogen.* **10**: 1–39
- 18 Nieuwkoop P. D., Johnen A. G. and Albers B. (1985) The Epigenetic Nature of Early Chordate Development: Inductive Interaction and Competence. Cambridge University Press, London
- 19 Nieuwkoop P. D. and Ubbels G. A. (1972) The formation of the mesoderm in urodelean amphibians IV. Qualitative evidence for the purely 'ectodermal' origin of the entire mesoderm and of the pharyngeal endoderm. *Roux. Arch. Entw. Org.* **169**: 185–199
- 20 Sudarwati S. and Nieuwkoop P. D. (1971) Mesoderm formation in the anuran *Xenopus laevis* Daudin. *Roux's Arch. Entw. Org.* **166**: 189–204
- 21 Asashima M. (1975) Inducing effects of the presumptive endoderm of successive stages in *Triturus alpestris*. *Roux's Arch. Dev. Biol.*, **177**: 301–308
- 22 Asashima M. (1994) Mesoderm induction during early amphibian development. *Review. Dev. Growth Differ.* **36**(4): 343–355
- 23 Nakamura O. and Toivonen S. (1978) In: Organizer – A milestone of a half-century from Spemann, pp. 1–379, Elsevier/North-Holland Biomedical Press, Amsterdam
- 24 New H. V., Howes G. and Smith J. C. (1991) Inductive interactions in early embryonic development. *Curr. Op. Genet. Dev.* **1**: 196–203
- 25 Hausen P. and Riebesell M. (1990) The Early Development of *Xenopus laevis*. An atlas of the histology. Springer-Verlag, Berlin
- 26 Nieuwkoop P. D. and Faber J. (1975) Normal table of *Xenopus laevis* (Daudin), 2nd ed., North-Holland Publ. Comp. Amsterdam
- 27 Ubbels G. A., Reijnen M., Meijerink J. and Narraway J. (1994) *Xenopus laevis* embryos can establish their spatial bilateral symmetrical body pattern without gravity. *Adv. Space. Res.* **14**: (8)257–(8)269
- 28 Ubbels G. A., Reijnen M., Meijerink J. and Narraway J. (1994) The role of gravity in the establishment of the dorso-ventral axis in the amphibian embryo (05-NL-EGGS). In: Biorack on IML-1 ESA-SP-1162: 175–185
- 29 Spemann H. (1938) Embryonic Development and Induction. Yale University Press, New Haven
- 30 Melton D. (1987) Translocation of a localized maternal mRNA to the vegetal pole of *Xenopus* oocytes. *Nature* **328**: 80–82
- 31 Melton D. A. (1991) Pattern formation during early development. *Science* **252**: 234–241
- 32 Smith W. C. and Harland R. M. (1992) Expression cloning of noggin, a new dorsaling factor localized to the Spemann organizer in *Xenopus* embryos. *Cell* **70**: 829–840
- 33 Smith W. C., Knecht A. K., Wu M. and Harland R. M. (1993) Secreted noggin protein mimics the Spemann organizer in dorsaling *Xenopus* mesoderm. *Nature* **361**: 547–549
- 34 Ruiz i Altaba A. and Melton D. A. (1990) Axial patterning and the establishment of polarity in the frog embryo. *Trends Genet.* **6**: 57–64
- 35 Dumont J. N. (1972) Oogenesis in *Xenopus laevis* (Daudin). I. Stages of oocyte development in laboratory maintained animals. *J. Morphol.* **136**: 153–180
- 35a Beetschen J.-C. and Daguzan C. (1993) Fécondation et développement d'ovocytes déjà pourvus d'un croissant gris expérimentalement formé pendant leur maturation. *C. R. Acad. Sci. Paris, Sciences de la vie/Life sciences*, **316**: 730–735
- 35b Smith L. D., Weilong X. and Varnold R. L. (1991) Oogenesis and oocyte isolation. In: *Methods in Cell Biology*, vol. 36, pp. 45–60, Kay B. K. and Peng H. B. (eds), Academic Press, San Diego.
- 36 Ding D. and Lipshitz H. D. (1993) Localized RNAs and their functions. *BioEssays* **15**: 651–658
- 37 Hauptman R. J., Perry B. A. and Capco D. G. (1989) A freeze-sectioning method for preparation of the detergent-resistant cytoskeleton identifies stage-specific cytoskeletal proteins and associated mRNA in *Xenopus* oocytes and embryos. *Dev. Growth Differ.* **31**: 157–164
- 38 Hesketh J. (1994) Translocation and the cytoskeleton: A mechanism for targeted protein synthesis. *Mol. Biol. Rep.* **19**: 233–243
- 39 Sardet C., McDougall A. and Houliston E. (1994) Cytoplasmic domains in eggs. *Trends Cell Biol.* **4**: 166–171
- 40 Vize P. D. and Thomsen G. H. (1994) Vg1 and regional specification in vertebrates: a new role for an old molecule. *Trends Genet.* **10**: 371–376
- 41 Gimlich R. L. and Gerhart J. C. (1984) Early cellular interactions promote embryonic axis formation in *Xenopus laevis*. *Dev. Biol.* **104**: 117–130
- 42 Imoh H. (1984) Appearance and distribution of RNA-rich cytoplasm in the embryo of *Xenopus laevis* during early development. *Dev. Growth Differ.* **26**: (1984) 167–176
- 43 Kageura H. (1990) Spatial distribution of the capacity to initiate a secondary embryo in the 32-cell embryo of *Xenopus laevis*. *Dev. Biol.* **142**: 432–438
- 44 Kageura H. and Yamana K. (1983) Pattern regulation in isolated halves and blastomeres of early *Xenopus laevis*. *J. Embryol. Exp. Morphol.* **74**: 221–234
- 45 Kageura H. and Yamana K. (1984) Pattern regulation in defect embryos of *Xenopus laevis*. *Dev. Biol.* **101**: 410–415
- 46 Kageura H. and Yamana K. (1986) Pattern formation in 8-cell composite embryos of *Xenopus laevis*. *J. Exp. Embryol. Exp. Morphol.* **91**: 79–100
- 47 Kinoshita K., Besho T. and Asashima M. (1993) Competence prepattern in the animal hemisphere of the 8-cell-stage *Xenopus* embryo. *Dev. Biol.* **160**: 276–284
- 48 Kinoshita K., Besho T. and Asashima M. (1995) Onset of competence to respond to activin A in isolated eight-cell stage *Xenopus* animal blastomeres. *Dev. Growth Differ.* **37**: 303–309

- 49 Danilchik M. V. and Gerhart J. C. (1987) Differentiation of the animal-vegetal axis in *Xenopus laevis* oocytes. 1) Polarized intracellular translocation of platelets establishes the yolk gradient. *Dev. Biol.* **122**: 101–112
- 50 Gerhart J., Danilchik M., Roberts J., Rowing B. and Vincent J.-P. (1986) Primary and Secondary Polarity of the Amphibian Oocyte and Egg. In: *Gametogenesis and the Early Embryo*, pp. 305–319, Ed. Alan R. Liss Inc.
- 51 Klag J. J. and Ubbels G. A. (1975) Regional morphological and cytochemical differentiation in the fertilized egg of *Discoglossus pictus* (Anura). *Differentiation* **3**: 15–20
- 52 Ancel P. and Vintemberger P. (1948) Recherches sur le déterminisme de la symétrie bilatérale dans l'oeuf des Amphibiens. *Bull. Biol. Fr. Belg. (suppl)* **31**: 1–182
- 53 Ortolani G. and VanderHaeghe F. (1965) L'activation de l'oeuf de *Xenopus laevis*. *Rev. Suisse Zool.* **72**: 652
- 54 Kirschner M. W., Gerhart J. C., Hara K. and Ubbels G. A. (1980) Initiation of the cell cycle and establishment of bilateral symmetry in *Xenopus* eggs. In: *The cell surface mediator of developmental processes*, Subtelny S. and Wessels K. (eds.), 38th Symp. *Dev. Biol.* **38**: 187–215
- 55 Morgan T. (1904) The dispensibility of the constant action of gravity and of a centrifugal force in the development of the toad's egg. *Anat. Anz.*, **25**: 94–96
- 56 Pasteels J. (1964) The morphogenetic role of the cortex of the amphibian egg. *Adv. Morphogen.* **3**: 363–388
- 57 Pflüger E. (1883) Über den Einfluss der Schwerkraft auf die Teilung der Zellen und auf die Entwicklung des Embryo. *Archiv.f.die gesamte Physiologie* **32**: 1–79
- 58 Roux W. (1884) Über die Entwicklung der Froscheier bei Aufhebung der richtenden Wirkung der Schwere. *Breslau Embryo.* 4. Die Richtungsbestimmung der Medianebene des Froschembryo durch die Kopulationsrichtung des Eikernes und des Spermakernes. *Arch. Mikrosk. Anat.* **29**: 157–212
- 60 Fautrez J. (1977) Effects of Space Environment on organism development. In: *Proc. European Symposium on Life Sciences Res. in Space*, ESA SP-130: 299–303
- 61 Ubbels G. A. (1988) The role of gravity in the establishment of the dorso-ventral axis in the amphibian embryo. In: *Biorack on spacelab D1 January 1988*, ESA-SP-1091: 147–155
- 62 Ubbels G. A. and Brom T. G. (1984) Cytoskeleton and Gravity at work in the establishment of Dorso-ventral polarity in the egg of *Xenopus laevis*. *Adv. Space Res.* **4**: (12)9–(12)18
- 63 De Mazière A., Gonzalez-Jurado J., Reijnen M., Narraway J. and Ubbels G. A. (1996) Transient effects of microgravity on early embryos of *Xenopus laevis*. *Adv. Space Res.*, **17**: (6/7)219–(6/7)223
- 64 Ubbels G. A., Berendsen W., Kerkvliet S. and Narraway J. (1990) Fertilization of *Xenopus* eggs in Space, In: *Proc. 4th Symp. on Life Sciences Res. in Space*, pp. 249–254, David V. (ed.), ESA Publ. SP-307: Trieste-Italy
- 65 Ubbels G. A., Berendsen W., Kerkvliet S. C. J. and Narraway J. M. (1991) Fertilization and Development of Eggs of the South African Clawed yoad *Xenopus laevis*, on Sounding Rockets in Space. *Adv. Space Res.* **12**: (1)181–(1)194
- 65a Ubbels G. A. (1977) Fertilisation and Development of *Xenopus* eggs on Sounding Rockets. In: *Biology on Sounding Rockets*. ESA SP 1206 (in press)
- 66 Black S. D. and Gerhart J. C. (1986) High frequency twinning of *Xenopus laevis* embryos from eggs centrifuged before first cleavage. *Dev. Biol.* **116**: 228–240
- 67 Neff A. W., Wakahara M. and Malacinski G. M. (1990) Bifurcation of the embryo's axis: analysis of variation in response to egg centrifugation. *Int. J. Dev. Biol.*, **34**: 391–398
- 68 Neff A. W., Yokota H., Chung H. M., Wakahara M. and Malacinski G. M. (1993) Early Amphibian (anuran) morphogenesis is sensitive to novel gravitational fields. *Dev. Biol.* **155**: 270–274
- 69 Souza K. A., Black S. D. and Wassersug R. J. (1995) Amphibian development in the virtual absence of gravity. *Proc. Natl. Acad. Sci. USA* **92**: 1975–1978
- 70 Brown E. E., Margelot K. M. and Danilchik M. V. (1994) Provisional bilateral symmetry in *Xenopus* eggs is established during maturation. *Zygote* **2**: (August) 213–220
- 71 Charbonneau M. and Grandin N. (1989) The egg of *Xenopus laevis*: a model system for studying cell activation. *Cell Differ. Dev.* **28**: 71–94
- 72 Dent J. A. and Klymkowsky M. W. Whole-mount analyses of cytoskeletal reorganization and function during oogenesis and early embryogenesis in *Xenopus*. In: *The Cell Biology of Fertilization*, pp. 63–103, Schatten H. and Schatten G. (eds), Acad. Press, San Diego
- 73 Elinson R. P. and Houliston E. (1990) Cytoskeleton in *Xenopus* oocytes and eggs. *Seminars in Cell Biol.* **1**: 349–377
- 74 Gard D. L. (1994) γ -Tubulin is asymmetrically distributed in the cortex of *Xenopus* oocytes. *Dev. Biol.* **161**: 131–140
- 75 Houliston E. and Elinson R. P. (1991) Patterns of microtubule polymerization relating to cortical rotation in *Xenopus laevis* eggs. *Development* **112**: 107–117
- 76 King M. L. and Barklis E. (1985) Regional distribution of maternal messenger RNA in the amphibian oocyte. *Dev. Biol.* **112**: 203–212
- 77 Paleček J., Habrová V., Nedvídek J. and Romanovský A. (1985) Dynamics of tubulin structures in *Xenopus laevis* oogenesis. *J. Embryol. Exp. Morphol.* **87**: 75–86
- 78 Brachet J., Hanocq F. and van Gansen P. (1970) A cytochemical and ultrastructural analysis of in vitro maturation in amphibian oocytes. *Dev. Biol.* **21**: 157–195
- 78a Huchon D., Crozet N., Cantenot N. and Ozon R. (1981) Germinal vesicle breakdown in the *Xenopus laevis* oocyte: Description of a transient microtubular structure. *Reprod. Nutr. Dev.* **21**: 135–148
- 79 Brachet J. (1979) Oogenesis and maturation in amphibian oocytes. *Endeavour* **3**: 144–149
- 80 Rebagliati M. R. and Dawid I. B. (1993) Expression of activin transcripts in follicle cells and oocytes of *Xenopus laevis*. *Dev. Biol.* **159**: 574–580
- 81 Gard D. L. (1991) Organization, nucleation and acetylation of microtubules in *Xenopus laevis* oocytes: A study by confocal immunofluorescence microscopy. *Dev. Biol.* **143**: 346–362
- 82 Ubbels G. A. and Vermeulen J. W. A. H. Dynamics of intracellular structure and cell determination during early development. *Acta Histochemica, Suppl.* **32**: (1986) 11–19
- 82a Paleček J. and Ubbels G. A. (1997) Dynamic changes in the tubulin cytoskeleton during oogenesis and early development in the anuran amphibian *Xenopus laevis* (Daudin). *Folia Histochem.* **35**: 3–18
- 83 Tourte M., Mignotte F. and Mounolou J.-C. (1984) Heterogeneous distribution and replication activity of mitochondria in *Xenopus laevis* oocytes. *Eur. J. Cell Biol.* **34**: 171–178
- 83a Kilmartin J. V., Wright B. and Milstein C. (1982) Rat monoclonal anti-tubulin antibodies derived by using a new non-secreting rat cell line. *J. Cell. Biol.* **93**: 576–582
- 84 Herkovits J. and Ubbels G. A. (1979) The ultrastructure of the dorsal yolk-free cytoplasm and the immediately surrounding cytoplasm in the symmetrized egg of *Xenopus laevis*. *J. Embryol. Exp. Morphol.* **51**: 155–164
- 85 Paleček J., Ubbels G. A. and Machá J. (1982) An immunocytochemical method for the visualization of tubulin-containing structures in the egg of *Xenopus laevis*. *Histochemistry* **76**: 527–538
- 86 Ubbels G. A., Machá J., Paleček J. and Koster C. H. (1983) Staining of actin and tubulin in sections of the uncleaved egg of *Xenopus laevis*, using the PAP method. In: *Progress in cell cycle controls*, 6th European Cell Cycle Workshop April 4–8, Chaloupka J., Kotyk A. and Striblova E. (eds), Czechoslovak Acad. Sci., Prague
- 87 Forristall C., Pondel M., Chen L. and King M. L. (1995) Patterns of localization and cytoskeletal association of two vegetally localized RNAs Vg1 and Xcat2. *Development* **121**: 201–208
- 88 Mosquera L., Forristall C., Zhou Y. and King M. L. (1993) A mRNA localized to the vegetal cortex of *Xenopus* oocytes encodes a protein with a nanos-like zinc finger domain. *Development* **117**: 377–386
- 89 Opresko L. K. Vitellogenin uptake and in vitro culture of oocytes, In: *Methods in Cell Biology, Xenopus laevis*: practical

- uses in cell and molecular biology, vol. 36, pp. 117–132, Kay B. K. and Peng H. B. (eds), Acad. Press, San Diego
- 90 Balbiani E. G. (1864) C. R. Hebd Séances Acad. Sci. **5**: 584
- 91 Guraya S. (1979) Recent advances in the morphology, cytochemistry and function of Balbiani's vitelline body in animal oocytes. *Int. Rev. Cytol.* **29**: 249–321
- 91a Schatten G. (1994) The centrosome and its mode of inheritance: The reduction of the centrosome during gametogenesis and its restoration during fertilization. *Dev. Biol.* **165**: 299–335
- 92 Billett F. S. and Adam E. (1976) The structure of the mitochondrial cloud of *Xenopus laevis* oocytes. *J. Embryol. Exp. Morphol.* **33**: 697–710
- 93 Coggins L. W. (1973) An ultrastructural and radioautographic study of early oogenesis in the toad *Xenopus laevis*. *J. Cell Sci.* **12**: 71–93
- 94 Heasman J., Quarmby J. and Wylie C. C. (1984) The mitochondrial cloud of *Xenopus* oocytes: the source of germinal granule material. *Dev. Biol.* **105**: 458–469
- 94a Mignotte F., Tourte M. and Mounolou J.-C. (1987) Segregation of mitochondria in the cytoplasm of *Xenopus* vitellogenic oocytes. *Biol. Cell* **60**: 97–102
- 95 Yost H. J., Phillips C. R., Boore J. L., Bertman J., Whalon B. and Danilchik M. V. (1995) Relocation of mitochondria to the prospective dorsal marginal zone during *Xenopus* embryogenesis. *Dev. Biol.* **170**: 83–90
- 96 Danilchik M. V. and Denegre J. M. (1991) Deep cytoplasmic rearrangements during early development in *Xenopus laevis*. *Development* **111**: 845–856
- 96a Paleček, J. and Romanovský A. (1985) Detection of tubulin structures of animal tissues in paraffin sections by immunofluorescence. *Histochem. J.* **17**: 519–521
- 97 Gard D. L. L., Affleck D. and Error B. M. (1995) Microtubule organisation, acetylation and nucleation in *Xenopus laevis* oocytes: II. A developmental transition in microtubule organisation during early diplotene. *Dev. Biol.* **168**: 189–201
- 97a Stearns T., Evans L. and Kirschner, M. (1991) γ -Tubulin is a highly conserved component of the centrosome. *Cell* **65**: 825–836
- 98 Kellogg D. R., Moritz M. and Alberts B. M. (1994) The centrosome and cellular organization. *Ann. Rev. Biochem.* **63**: 639–674
- 99 Kloc M. and Etkin L. D. (1995) Two distinct pathways for the localization of RNAs at the vegetal cortex in *Xenopus* oocytes. *Development* **121**: 287–297
- 100 Yisraeli J. K., Sokol S. and Melton D. A. (1989) The process of localizing a maternal messenger RNA in *Xenopus* oocytes. *Development suppl.* **107**: 31–36
- 101 Yisraeli J. K., Sokol S. and Melton D. A. (1990) A two step model for the localization of maternal mRNA in *Xenopus* oocytes: Involvement of microtubules and microfilaments in translocation and anchoring of Vg1 mRNA. *Development* **108**: 289–298
- 102 Thomsen G. and Melton D. A. (1993) Processed Vg1 protein is an axial mesoderm inducer in *Xenopus*. *Cell* **74**: 433–441
- 103 Elinson R. P., King M. L. and Forristall C. (1993) Isolated vegetal cortex from *Xenopus* oocytes selectively retains localized mRNAs. *Dev. Biol.* **160**: 554–562
- 103a Mowry K. and Melton D. (1992) Vegetal messenger RNA localization directed by a 340nt sequence element in *Xenopus* oocytes. *Science* **255**: 991–993
- 103b Wilhelm J. E. and Vale R. D. (1993) RNA on the move: The mRNA localization pathway. Mini-Review, *J. Cell Biol.* **123**: 269–274
- 104 Elinson R. P. (1980) The amphibian egg cortex in fertilization and early development. *Symp. Dev. Biol.* **38**: 217–234
- 105 Hara K., Tydeman P. and Kirschner M. (1980) A cytoplasmic clock with the same period as the division cycle in the *Xenopus* egg. *Proc. Natl. Acad. Sci. (USA)* **77**: 462–466
- 105a Chow R. L. and Elinson R. P. (1993) Local alteration of cortical actin in *Xenopus* eggs by the fertilizing sperm. *Molec. Reprod. Devel.* **35**: 69–75
- 106 Ubbels G. A. (1988) A first fertilization of frog eggs in space. *Microgravity News from ESA* **1/2**: 19–23
- 107 Elinson R. P. and Paleček J. (1993) Independence of two microtubule systems in fertilized frog eggs: the sperm aster and the vegetal parallel array. *Roux's Arch. Dev. Biol.* **202**: 224–232
- 108 Wilson E. B. (1925) *The cell in development and heredity*; Third ed. MacMillan, New York
- 109 Klymkowski M. W. and Karnovski A. (1994) Morphogenesis and the cytoskeleton: Studies of the *Xenopus* embryo. *Dev. Biol.* **165**: 372–384
- 110 Elinson R. P. and Rowning B. (1988) A transient array of parallel microtubules in frog eggs: Potential tracks for a cytoplasmic rotation that specifies the dorso-ventral axis. *Dev. Biol.* **128**: 185–197
- 111 Briedis A. and Elinson R. P. (1982) Suppression of male pronuclear movement in frog eggs by hydrostatic pressure and deuterium oxide yields androgenetic haploids. *J. Exp. Zool.* **222**: 45–57
- 112 Elinson R. P. (1985) Changes in levels of polymeric tubulin associated with activation and dorsoventral polarization of the frog egg. *Dev. Biol.* **109**: 224–233
- 113 Kirschner M. and Mitchison T. (1986) Beyond self-assembly: from microtubules to morphogenesis. *Cell* **45**: 329–342
- 114 Vale R. D. (1991) Severing of stable microtubules by a mitotically activated protein in *Xenopus* egg extracts. *Cell* **64**: 827–839
- 115 Vandekerckhove J. (1990) Actin-binding proteins. *Curr. Op. Cell Biol.* **2**: 41–50
- 116 Walker R. A., O'Brien E. T., Pryer N. K., Soboeiro M. F., Voter W. A., Erickson H. P. et al. (1988) Dynamic instability of individual microtubules analysed by video light microscopy: Rate constants and transition frequencies. *J. Cell Biol.* **107**: 1437–1448
- 117 Pestell R. Q. W. (1975) Microtubular protein synthesis during oogenesis and early embryogenesis in *Xenopus laevis*. *Biochem. J.* **145**: 527–534
- 117a Perry B. A. and Capco D. G. (1988) Spatial reorganization of actin, tubulin, and histone mRNAs during meiotic maturation and fertilization in *Xenopus* oocytes. *Cell Differ.* **25**: 99–108
- 118 Chu D. T. W. and Klymkowsky M. W. (1989) The appearance of acetylated α -tubulin during early development and cellular differentiation in *Xenopus*. *Dev. Biol.* **136**: 104–117
- 119 Vincent J. P. and Gerhart J. C. (1987) Subcortical rotation in *Xenopus* eggs: an early step in embryonic axis specification. *Dev. Biol.* **123**: 526–539
- 120 Vincent J.-P., Oster G. F. and Gerhart J. C. (1986) Kinematics of grey crescent formation in *Xenopus* eggs: The displacement of subcortical cytoplasm relative to the egg surface. *Dev. Biol.* **113**: 484–500
- 121 Vincent J.-P., Scharf S. R. and Gerhart J. C. (1987) Subcortical rotation in *Xenopus* eggs: A preliminary study of its mechanochemical basis. *Cell Motil. Cytoskel.* **8**: 143–154
- 122 Schroeder M. M. and Gard D. L. (1992) Organization and regulation of cortical microtubules during the first cell cycle of *Xenopus* eggs. *Development* **114**: 699–709
- 123 Houliston E. (1994) Microtubule translocation and polymerization during cortical rotation in *Xenopus* eggs. *Development* **120**: 1213–1220
- 124 Belmont L. D., Hyman A. A., Sawin K. E. and Mitchison T. J. (1990) Real-time visualization of cell-cycle dependent changes in microtubule dynamics in cytoplasmic extracts. *Cell* **62**: 579–589
- 125 Houliston E. and Elinson R. P. (1991) Evidence for the involvement of microtubules, ER and kinesin in the cortical rotation of fertilized frog eggs. *J. Cell Biol.* **114**: 1017–1028
- 126 Houliston E. and Elinson R. P. (1992) Microtubules and cytoplasmic reorganization in the frog egg. *Curr. Top. Dev. Biol.* **26**: 53–70
- 127 Scharf S. R., Rowning B., Wu M. and Gerhart J. C. (1989) Hyperdorsoanterior embryos from *Xenopus* eggs treated with D₂O. *Dev. Biol.* **134**: 175–188
- 128 Hiradhar P. K. and Ubbels G. A. (1987) Axis derangement in *Xenopus laevis* through nocodazole and deuterium oxide treatments. *Cell Diff. suppl.* **20**: 45S

- 129 Black S. D. and Vincent J. P. (1988) The first cleavage plane and the embryonic axis are determined by separate mechanisms in *Xenopus laevis*, II. Experimental dissociation by lateral compression of the egg. *Dev. Biol.* **128**: 65–71
- 130 Danilchik M. V. and Black S. D. (1988) The first cleavage plane and the embryonic axis are determined by separate mechanisms in *Xenopus laevis*, I. Independence in undisturbed embryos. *Dev. Biol.* **128**: 58–64
- 131 Bauer D. V., Huang S. and Moody S. A. (1994) The cleavage stage origin of Spemann's organizer: analysis of the movements of blastomere clones before and during gastrulation in *Xenopus*. *Development* **120**: 1179–1189
- 131a Bauer D. V., Best D. W., Hainski A. M. and Moody S. A. (1996) A Contact-Dependent Animal to Vegetal Signal Biases Neural Lineages during *Xenopus* Cleavage Stages. *Dev. Biol.* **178**: 217–228
- 132 Keller R. E. (1980) The cellular basis of epiboly: An SEM study of deep-cell rearrangement during gastrulation in *Xenopus laevis*. *J. Embryol. Exp. Morphol.* **60**: 201–234
- 132a Vodicka M. A. and Gehart J. C. (1995) Blastomere derivation and domains of gene expression in the Spemann Organizer of *Xenopus laevis*. *Development* **121**: 3505–3518
- 133 Sokol S. Y. and Melton D. A. (1991) Preexistent pattern in *Xenopus* animal pole cells revealed by induction with activin. *Nature*, **351**: 409–411
- 134 Sokol S. Y. and Melton D. A. (1992) Interaction of Wnt and activin in dorsal mesoderm induction in *Xenopus*. *Dev. Biol.* **154**: 348–355
- 135 Saint-Jeannet, J.-P. and Dawid I. B. (1994) A fate map for the 32-cell stage of *Rana pipiens*. *Dev. Biol.* **166**: 755–762
- 136 Yuge M., Kobayakawa Y., Fujisue M. and Yamana K. (1990) A cytoplasmic determinant for dorsal axis formation in an early embryo of *Xenopus laevis*. *Development* **110**: 1051–1056
- 137 Brachet J. (1938) La localisation des protéines sulfhydrylées pendant le développement des Amphibiens. *Bull. Acad. r. Belg. Cl. Sci.* 449–510
- 138 Denegre J. M. and Danilchik M. V. (1993) Deep cytoplasmic rearrangements in axis-respecified *Xenopus* embryos. *Dev. Biol.* **160**: 157–164
- 139 Brown E. E., Denegre J. M. and Danilchik M. V. (1993) Deep cytoplasmic rearrangements in ventralized *Xenopus* embryos. *Dev. Biol.* **160**: 148–156
- 140 Child C. M. (1929) Physiological dominance and physiological isolation in development and reconstitution. *Roux. Arch. Entwickl. mech.* **117**: 21–66
- 141 Curtis A. S. G. (1960) Cortical grafting in *Xenopus laevis*. *J. Embryol. Exp. Morphol.* **8**: 163–173
- 142 Curtis A. S. G. (1962) Morphogenetic interactions before gastrulation in the amphibian *Xenopus laevis*. The cortical field. *J. Embryol. Exp. Morphol.* **10**: 410–422
- 143 Cooke J. (1986) Permanent distortion of positional system of *Xenopus* embryo by brief early perturbation in gravity. *Nature* **319**: 60–63
- 143a Melton D. A. and Rebagliati M. R. (1986) Anti-sense RNA injections in fertilized eggs as a test for the function of localized mRNAs. *J. Embryol. Exp. Morphol.* **97**: suppl. 211–221
- 144 Elinson R. P. and Pasceri P. (1989) Two UV-sensitive targets in dorsoanterior specification of frog embryos. *Development* **106**: 511–518
- 145 Holowacz T. and Elinson R. P. (1993) Cortical cytoplasm, which induces dorsal axis formation in *Xenopus*, is inactivated by UV irradiation of the oocyte. *Development* **119**: 277–285
- 146 Holowacz T. and Elinson R. P. (1995) Properties of the dorsal activity found in the vegetal cortical cytoplasm of *Xenopus* eggs. *Development* **121**: 2789–2798
- 147 Malacinski G. M., Benford H. and Chung H. M. (1975) Association of an ultraviolet irradiation sensitive cytoplasmic localization with the future dorsal side of the amphibian egg. *J. Exp. Zool.* **191**: 97–110
- 148 Mise N. and Wakahara M. (1994) Dorsoventral polarization and formation of dorsal axial structures in *Xenopus laevis*: analyses using UV irradiation of the full-grown oocyte and after fertilization. *Int. J. Dev. Biol.* **38**: 447–453
- 149 Scharf S. R. and Gerhart J. C. (1980) Determination of the dorso-ventral axis in eggs of *Xenopus laevis*: complete rescue of uv-impaired eggs by oblique orientation before first cleavage. *Dev. Biol.* **79**: 181–198
- 150 Scharf S. R. and Gerhart J. C. (1983) Axis determination in eggs of *Xenopus laevis*: A critical period before first cleavage, identified by the common effects of cold, pressure and ultraviolet irradiation. *Dev. Biol.* **99**: 75–87
- 150a Savage R. M. and Danilchik M. V. (1993) Dynamics of germ plasm localization and its inhibition by ultraviolet irradiation in early cleavage *Xenopus* embryos. *Dev. Biol.* **157**: 371–382
- 151 Wakahara M. (1989) Specification and establishment of dorso-ventral polarity in eggs and embryos of *Xenopus laevis*. *Dev. Growth Differ.* **31**: 197–207
- 152 Grunz H. (1994) The four animal blastomeres of the eight-cell stage of *Xenopus laevis* are intrinsically capable of differentiating into dorsal mesodermal derivatives. *Int. J. Dev. Biol.* **38**: 69–76
- 153 Takasaki H. and Konishi H. (1989) Dorsal blastomeres in the equatorial region of the 32-cell *Xenopus* embryo autonomously produce progeny committed to the organizer. *Dev. Growth Differ.* **31**(2): 147–156
- 154 Cardellini P. (1988) Reversal of dorsoventral polarity in *Xenopus laevis* embryos by 180° rotation of the animal micromeres at the eight-cell stage. *Dev. Biol.* **128**: 428–434
- 155 Wakahara M. (1986) Modification of dorso-ventral polarity in *Xenopus laevis* embryos following withdrawal of egg contents before first cleavage. *Dev. Growth Differ.* **28**: 543–554
- 156 Gurdon J. B., Mohun T. J., Fairman S. and Brennan S. (1985) All components required for the eventual activation of muscle specific actin genes are localized in the sub-equatorial region of an uncleaved amphibian egg. *Proc. Natl. Acad. Sci. USA*, **82**: (1985) 139–143
- 157 Zisckind N. and Elinson R. P. (1990) Gravity and microtubules in dorsoventral polarization of the *Xenopus* egg. *Dev. Growth Differ.* **32**: 575–581
- 158 Gimlich R. L. (1986) Acquisition of developmental autonomy in the equatorial region of the *Xenopus* embryo. *Dev. Biol.* **115**: 340–352
- 159 Gimlich R. L. and Cooke J. (1983) Cell lineage and the induction of second nervous systems in amphibian development. *Nature* **306**: 471–473
- 160 Hainski A. M. and Moody S. A. (1992) *Xenopus* maternal RNAs from a dorsal animal blastomere induce a secondary axis in host embryos. *Development* **116**: 347–355
- 161 Fujisue M., Kobayakawa Y. and Yamana K. (1993) Occurrence of dorsal-axis inducing activity around the vegetal pole of an uncleaved *Xenopus* egg and displacement to the equatorial region by cortical rotation. *Development* **118**: 163–170
- 162 Weeks D. L. and Melton D. A. (1987) A maternal mRNA localized to the vegetal hemisphere in *Xenopus* eggs codes for a growth factor related to TGF- β . *Cell* **51**: 861–867
- 163 Kessler D. S. and Melton D. A. (1995) Induction of dorsal mesoderm by soluble, mature Vg1 protein. *Development* **121**: 2155–2164
- 164 Elinson R. P. and Kao K. R. (1989) The location of dorsal information in frog early development. *Dev. Growth Differ.* **31**: 423–430
- 165 Yokota H., Neff A. W. and Malacinski G. M. (1992) Altering the position of the first horizontal cleavage furrow of the amphibian (*Xenopus*) egg reduces embryonic survival. *Int. J. Dev. Biol.* **36**: 527–535
- 166 Cogoli A., Bechler B., Cogoli-Greuter M., Criswell S. B., Joller H., Joller P. et al. (1993) Mitogenic signal transduction in T lymphocytes in microgravity. *J. Leucoc. Biol.* **53**: 569–575
- 167 Cogoli A., Iversen T. H., Johnsson A., Mesland D. and Oser H. (1989) Cell Biology. In: Life Sciences Research in Space. ESA SP-1105: 49–64
- 168 McLaren A. (1989) Developmental Biology. In: Life Sciences Research in Space. ESA SP-1105: 31–36

- 169 Lapchine L., Moatti N., Gasset G., Richoille G., Templier J. and Tixador R. (1986) Antibiotic activity in Space. *Drugs Exptl. Clin. Res.* **2**: 933–938
- 170 Mennigmann H. D. and Lange M. (1986) Growth and differentiation of *Bacillus subtilis* under microgravity conditions. *Naturwissenschaften* **73**: 415–417
- 170a Bruschi C. V. and Esposito M. S. (1994) Cell division, mitotic recombination and onset of meiosis by diploid yeast cells during Space flight (US-2 YEAST). *ESA SP* **1162**: 83–93
- 171 Spooner B. S., Metcalf J., Debell L., Paulsen A., Noren W. and Guikema J. A. (1994) Development of the brine shrimp *Artemia* is accelerated during spaceflight. *J. Exp. Zool.* **269**: 253–262
- 172 Bechler B., Cogoli A., Cogoli-Greuter M., Muller O., Hunzinger E. and Crisswell S. B. (1992) Activation of microcarrier-attached lymphocytes in microgravity. *Biotech. and Bioeng.* **40**: 991–996
- 172a Spooner B. S., Hardman P. and Paulsen A. (1994) Gravity in mammalian organ development: Differentiation of cultured lung and pancreas rudiments during spaceflight. *J. Exp. Zool.* **269**: 253–262
- 173 Moos P. J., Fattaey H. K. and Johnson T. C. (1994) Cell proliferation inhibition in reduced gravity. *Exp. Cell Res.* **213**: 458–462
- 174 Groot R. P. de, Rijken P. J., Den Hertog J., Boonstra J., Verkleij A. J., De Laat S. W. et al. (1991) Nuclear responses to protein kinase C signal transduction are sensitive to gravity changes. *Exp. Cell Res.* **197**: 87–90
- 174a Young R. S. and Tremor J. W. (1968) Session III: The effect of weightlessness on the dividing egg of *Rana pipiens*. *Bio Science* **18**: 609–615
- 175 Ubbels G. A., Berendsen W., Kerkvliet S. and Narraway J. (1989) The first seven minutes of a *Xenopus* egg fertilized on a Sounding Rocket in Space. In: *Microgravity as a tool in developmental biology*. Guyennet D. (ed.), Special Symposium at the 11th International congress of the International Society of Developmental Biologists. *ESA-SP-1123*: 49–58
- 176 Ubbels G. A., Berendsen W. and Narraway J. M. (1989) Fertilization of frog eggs on a Sounding Rocket in Space. *Adv. Sp. Res.* **9**: (11)187–(11)197
- 177 Verhoeff-de Fremery R. and Vervoordeldonk, F. J. M. (1982) Skin autografts as markers in the toad *Xenopus laevis*. *Laboratory Animals* **16**: 156–158
- 178 Ubbels G. A. and Willemsen H. P. (1989) Automatic experiment container (AEC) for fertilization of frog eggs in Space. A multipurpose piece of classified Space hardware. In: *Microgravity as a tool in developmental biology*. Special Symposium at the 11th International congress of the International Society of Developmental Biologists. *ESA-SP-1123*: 75–78
- 179 Wakahara M., Neff A. W. and Malacinski G. M. (1985) Development of delayed gastrulae and permanent blastulae from inverted *Xenopus laevis* eggs. *Acta Embryol. Morph. Exp.*, **6**: 193–209
- 180 Chung Hae-Moon, Yokota H., Dent A., Malacinski G. M. and Neff A. W. (1994) The location of the third cleavage plane of *Xenopus* embryos partitions morphogenetic information in animal quartets. *Int. J. Dev. Biol.* **38**: 421–428
- 181 Klymkowski M. W. and Hanken J. (1991) Whole-mount staining of *Xenopus* and other vertebrates. In: *Methods in Cell Biology* vol. 36, pp. 419–441, Kay B. K. and Peng H. B. (eds) Academic Press, San Diego
- 182 De Mazière A. M., Hage W. J. and Ubbels G. A. (1996) A method for staining of cell nuclei, in *Xenopus laevis* embryos, with cyanine dyes for whole-mount confocal laser scanning microscopy. *J. Histochem. Cytochem.* **44**: 399–402
- 183 Han Y., Pralong-Zamofing D., Ackermann U. and Geering K. (1991) Modulation of N_a^+ , K-ATPase expression during early development of *Xenopus laevis*. *Dev. Biol.* **145**: 174–181
- 184 Viklický V., Dráber P., Hašek J. and Bártek J. (1982) Production and characterization of a monoclonal antitubulin antibody. *Cell Biol. Int. Rep.* **6**: 725–731
- 185 Simionescu N. and Simionescu M. (1976) Galloylglucoses of low molecular weight as mordant for electron microscopy. I. Procedure and evidence for mordanting effect. *J. Cell Biol.* **70**: 608–621
- 186 Colman A. and Drummond D. (1986) The stability and movement of mRNA in *Xenopus* oocytes and embryos. *J. Embryol. Exp. Morphol.* **97**: Supplement, 197–209